Reviewed Preprint
v1 • September 15, 2026
Not revised

For correspondence:
maruyama-ck@igakuken.or.jp
kumamoto-tk@igakuken.or.jp

Competing interests: No competing interests declared

Funding: See page 35

Reviewing editor: Catherine Emily Carr, University of Maryland, United States

Mosaic evolution of avian brain compartments revealed by comparative MRI

Yuki Kawabe[1,2], Tomokazu Tsurugizawa[3,4,5], Chiaki Ohtaka-Maruyama[1] ✉, Takuma Kumamoto[1] ✉

[1]Developmental Neuroscience Project, Department of Brain and Neurosciences, Tokyo Metropolitan Institute of Medical Science, Tokyo, Japan • [2]Developmental Neurology, Molecular and Cellular Medicine Course, Niigata University Graduate School of Medical and Dental Sciences, Niigata, Japan • [3]National Institute of Advanced Industrial Science and Technology (AIST), Tsukuba, Japan • [4]Institute of Systems and Information Engineering, University of Tsukuba, Tsukuba, Japan • [5]Université du Québec à Trois-Rivières, Trois-Rivières, Canada

eLife Assessment

The main contribution of this potentially **useful** manuscript is a standardized comparative MRI resource covering multiple avian clades, complemented by histological cross-validation and diffusion-based connectivity analyses. Such a resource could significantly enhance accessibility to internal avian brain anatomy for evolutionary neurobiology. Its central claim that avian brain compartments exhibit modular diversification aligns with the existing literature. However, uncertainties regarding data availability, concerns with the tractography pipeline, and insufficient recognition of prior work lead to the conclusion that the methods, data, and analyses are **incomplete**.

https://doi.org/10.7554/eLife.112415.1.sa3

Abstract

Birds evolved large, cognitively capable forebrains independently of mammals, yet comparative analyses of avian brain organization have been constrained by the lack of standardized resources capable of resolving internal parcellation and long-range connectivity across species. Here, we present a comparative MRI resource spanning 16 avian species representing major clades and diverse ecological niches. We analyzed high-resolution T2-weighted and diffusion-weighted datasets suitable for direct interspecific comparison. T2-weighted morphometry revealed pronounced region-specific variation in internal brain architecture, including lineage-dependent differences in the relative prominence of major brain divisions and commissural structures, supporting a pattern of mosaic diversification rather than uniform scaling. To validate MRI-derived anatomical boundaries, we compared MRI parcellations with complementary histological analyses in three representative taxa (the large-billed crow, gentoo penguin, and mandarin duck), demonstrating close correspondence between MRI-defined borders and cytoarchitectonic transitions identified by Nissl staining, as well as major myelinated compartments visualized by Luxol Fast Blue staining. Moreover, diffusion MRI tractography and fractional anisotropy (FA) mapping further revealed both conserved and species-specific features of large-scale brain organization. Seed-based tractography of the optic lobe, dorsal cortex, cerebellum, and anterior cortex in chick, gentoo penguin, and large-billed crow revealed conserved within-compartment trajectory patterns alongside marked region-specific interspecific differences, particularly in optic-lobe-associated long-range trajectories. Whole-brain FA maps revealed complementary variation in regional microstructural organization across taxa. Together, this comparative MRI framework provides a cross-validated foundation for linking internal brain anatomy and long-range connectivity to ecological and evolutionary diversification in birds, with broader applications to comparative neuroanatomy across amniotes.

Significance Statement

How does the internal architecture of the brain reorganize as species adapt to diverse lifestyles? Traditional comparative neuroanatomy has largely relied on overall brain size and external morphology, providing limited insight into internal subdivisions and long-range connectivity. In this study, we present a standardized avian MRI resource and a reproducible analytical pipeline that enables direct cross-species comparisons of 3D morphometry and diffusion-derived connectivity across 16 bird species representing major clades and diverse ecological niches. MRI-derived anatomical boundaries are validated through complementary histological analyses, providing biological support for cross-species parcellation and white-matter measurements. Using this framework, we demonstrate that avian brains diversify in a strongly mosaic manner, with region-and pathway-specific changes that vary disproportionately across lineages rather than scaling uniformly with overall brain size. By moving beyond simple correlations between brain size and behavior, this resource provides a benchmark for testing hypotheses of mosaic brain evolution and for linking neural architecture to ecological and behavioral diversification across vertebrates.

Introduction

The overall organization of the vertebrate brain is broadly conserved, yet only a few lineages have undergone dramatic and repeated expansion of specific brain divisions. The telencephalon is a prominent example, having expanded extensively in both mammals and birds and representing two independent evolutionary routes to large, cognitively capable forebrains (1, 2).

Mammals evolved a laminated six-layer neocortex, whereas birds achieved comparable behavioral sophistication with a pallium that is predominantly nuclear in its cytoarchitecture (1, 3). This architectural divergence, despite partial functional convergence, makes birds a powerful comparative system for identifying general principles underlying forebrain enlargement and specialization across vertebrates (1, 4). Birds also display substantial diversity in ecological niches, sensory systems, social behaviors, and cognitive capacities across lineages (5–9). Such variation is thought to reflect mosaic scaling of pallial and subpallial regions, together with differences in long-range white-matter organization and interhemispheric integration. However, comparative studies of avian brain evolution have relied primarily on neuron-count scaling analyses and CT-based endocast reconstructions (3,10). Although these approaches have provided important insights into overall brain size and external morphology, they cannot resolve internal brain parcellation or long-range tract architecture. Consequently, the field still lacks harmonized, publicly available datasets and analytical frameworks for cross-species comparisons of internal brain organization and connectivity. Existing avian MRI resources have largely been limited to species-specific atlases or diffusion tensor imaging (DTI) studies focused on song systems, rather than comparative whole-brain datasets spanning multiple avian lineages (9, 11, 12).

Here, we address this gap by assembling a comparative MRI resource encompassing 16 bird species representing major avian clades and diverse ecological niches. The dataset combines 13 species from the Animal Brain Collection (ABC) with three publicly available datasets and applies a unified framework for structural, morphometric, and diffusion MRI analyses (11,13–16). Building on the ABC framework, we integrate high-resolution structural and diffusion MRI data acquired using harmonized protocols. We register brains to species-specific templates and a common comparative space, enabling quantification of regional volumes and morphology, relative investment across major brain divisions, white-matter macroarchitecture, and commissural organization. Using this framework, we evaluate three a priori predictions regarding avian neuroanatomical diversification. First, associative pallial territories exhibit disproportionate scaling in taxa with complex social behaviors. Second, white-matter volume and tract coherence covary with relative telencephalon size. Third, interhemispheric routing displays clade-specific scaling consistent with alternative architectural solutions for bilateral integration. Together, this

study provides a comparative MRI resource for birds and a reproducible framework for linking whole-brain anatomy and connectivity to ecological and behavioral diversification across avian lineages, with broader applicability to comparative neuroanatomy across vertebrates.

Results

MRI Analysis of a Comparative Structural MRI Resource Across Avian Taxa

First, we assembled a comparative avian MRI cohort comprising 12 species from the ABC (13) and four publicly available avian MRI datasets: canary (14), starling (16), pigeon (15), and zebra finch (11) (Fig. 1). The resulting dataset included 16 species representing four major avian groups: Galloanserae (green), Columbaves (purple), Aequorlitornithes (blue), and Inopinaves (orange). High-resolution T2-weighted and diffusion-weighted images were obtained for direct interspecific comparisons. Representative coronal sections demonstrated sufficient image quality and contrast to resolve internal anatomical landmarks across all taxa, providing a robust basis for subsequent morphometric and connectivity analyses (Fig. 1B).

Interspecific Diversity in Internal Brain Architecture

T2-weighted morphometry revealed substantial interspecific variation in the relative size, morphology, and configuration of major brain divisions. For example, the anterior commissure (AC) was readily identifiable in all 16 species but differed markedly in its relative prominence among taxa (Fig. 2A). The AC appeared particularly prominent in the large-billed crow, starling, and canary, whereas it was comparatively reduced in the mallard, mandarin duck, and crested partridge. Penguins also exhibited a relatively small AC, suggesting lineage-dependent differences in telencephalic interhemispheric pathways across species (Fig. 2A). However, quantitative analysis showed that AC area scaled approximately with whole-brain area across species (Fig. 2B), indicating that relative AC size varies little after normalization to overall brain size. In birds, the AC interconnects arcopallial and preoptic/anterior forebrain regions and can also link non-homotopic territories between hemispheres (17). Although AC size cannot be interpreted directly as a measure of processing complexity, it represents the principal commissural pathway connecting the two pallial hemispheres in birds. Collectively, these findings suggest that the apparent interspecific differences in AC prominence are largely attributable to variation in overall brain size within the present dataset. Thus, while the AC remains an important anatomical landmark for comparative studies of avian interhemispheric organization, our area-based analysis provides limited evidence for major lineage-specific differences in relative commissural investment.

Next, we examined interspecific variation in cerebellar development using sagittal sections, which allow detailed assessment of cerebellar structural complexity (Fig. 2C). Sagittal T2-weighted sections revealed clear differences in the overall size and folial organization of the cerebellum among species. The mallard, mandarin duck, crested partridge, black-necked stilt, and boat-billed heron exhibited fewer and less elaborate cerebellar folia, whereas the pigeon, large-billed crow, and toucan possessed larger and more densely foliated cerebella. To further anchor these MRI-based observations to tissue-level anatomy, representative histological sections were examined in selected species and showed corresponding differences in folial branching patterns and cerebellar structural complexity (Fig. 2D). Quantification of cerebellar folial branching revealed relatively little variation in the number of basal branches across species, whereas terminal branch number was substantially greater in penguins, toucans, and crows (Fig. 2E). This distinction between basal and terminal branches indicates that interspecific variation was most evident in distal folial elaboration rather than in the primary branching scaffold of the cerebellum. This pattern suggests that the primary cerebellar scaffold is comparatively conserved across the sampled taxa, whereas distal folial elaboration represents a more variable anatomical feature. Because cerebellar foliation increases the available cortical surface within the cerebellum, variation in terminal branching may reflect lineage-specific expansion of sensorimotor processing capacity, although

Figure 1. Avian species included in a comparative MRI dataset.

Overview of the 16 avian species included in this study, representing major avian clades and diverse ecological niches. (A) Phylogenetic relationships among the sampled species, grouped into four major avian lineages. (B) Representative coronal T2-weighted MRI sections and corresponding photographs of each species. These images illustrate the diversity of brain sizes and overall morphologies represented in the dataset and demonstrate sufficient internal contrast to identify major anatomical landmarks across taxa. All MRI datasets were processed using a standardized preprocessing workflow to enable direct cross-species comparisons.

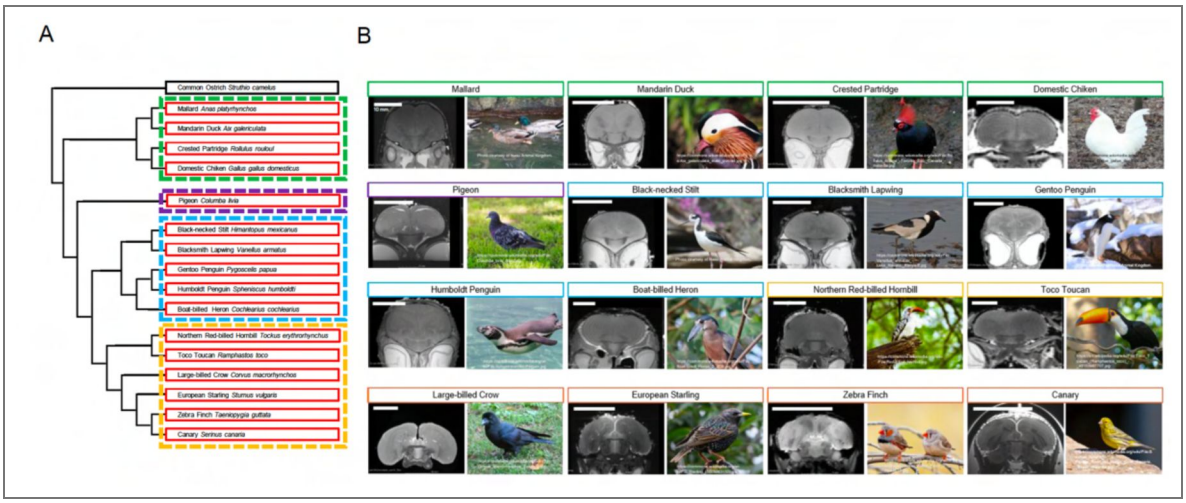

Table 1. Image sources for animal photographs used in Figure 1.

Name	Developmental stage	URL
Mallard	NA	Photo courtesy of Nasu Animal Kingdom.
Mandarin Duck	Adult	https://commons.wikimedia.org/wiki/File:Aix_galericulata_male_portrait.jpg
Crested Partridge	NA	https://commons.wikimedia.org/wiki/File:Rollulus_rouloul_-Toronto_Zoo,_Canada_-male-8a.jpg
Chicken	Adult	https://commons.wikimedia.org/wiki/File:Ma_-_Male_Gallus_gallus_domesticus_-_1.jpg
Pigeon	Adult	https://commons.wikimedia.org/wiki/File:Columba_livia_dove.jpg
Black-necked Stilt	NA	Photo courtesy of Nasu Animal Kingdom.
Blacksmith Lapwing	NA	https://commons.wikimedia.org/wiki/File:Vanellus_armatus_-Lake_Nakuru,_Kenya-8.jpg
Gentoo Penguin	NA	Photo courtesy of Nasu Animal Kingdom.
Humboldt Penguin	1w	https://commons.wikimedia.org/wiki/File:Schwimmender-Pinguin.jpg
Boat-billed Heron	Adult	https://commons.wikimedia.org/wiki/File:Boat-billed_Heron_2_JCB.jpg
Northern Red-billed Hornbill	Adult	https://commons.wikimedia.org/wiki/File:Red-billed_hornbill.jpg
Toco Toucan	Adult	https://en.wikipedia.org/wiki/File:Toco_Toucan_(Ramphastos_toco)_-_48153967707.jpg
Large-billed Crow	Adult	https://commons.wikimedia.org/wiki/File:Corvus_macrorhynchos_Tokyo_6.jpg
European Starling	Adult	https://commons.wikimedia.org/wiki/File:Starling_(5503763150).jpg
Zebra Finch	Adult	https://commons.wikimedia.org/wiki/File:Australian_Zebra_Finch_0A2A3013.jpg
Canary	Adult	https://commons.wikimedia.org/wiki/File:Serinus_canaria_-Parque_Rural_del_Nublo,_Gran_Canaria,_Spain_-male-8a.jpg
Egyptian Rousette	Adult	https://commons.wikimedia.org/wiki/File:Rousettus_aegyptiacus_185858.jpg

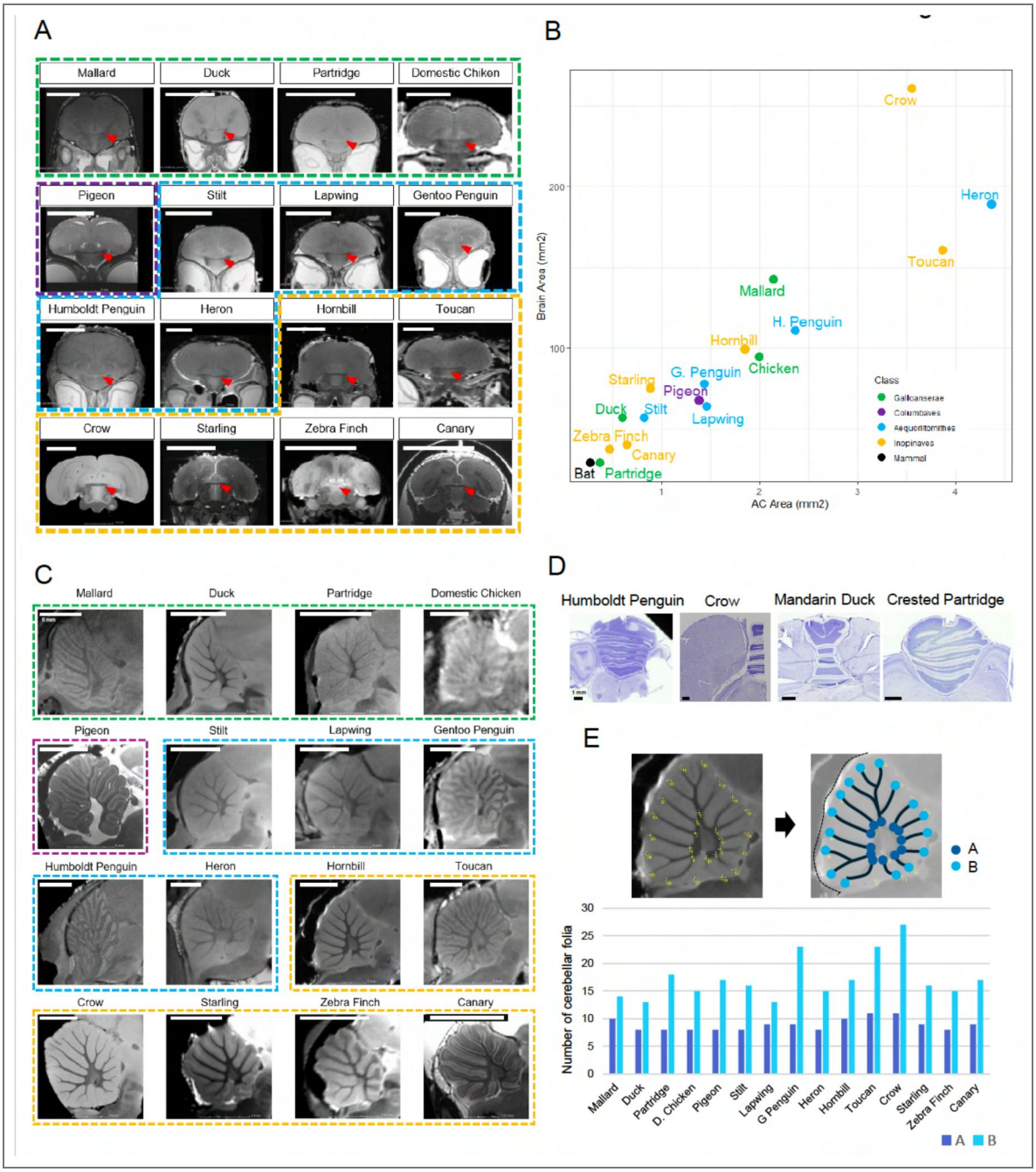

Figure 2. Whole-brain T2-weighted MRI highlights region-specific interspecific diversity in birds.

(A) Representative coronal T2-weighted images from multiple species reveal pronounced differences in the relative size and morphology of major brain divisions, as well as overall head morphology. The anterior commissure (AC), the principal interhemispheric commissure in birds, is readily identifiable across taxa (red arrows). (B) Quantification of AC size relative to whole-brain area across species. AC area scales approximately with brain size, indicating that apparent differences in AC prominence largely reflect variation in overall brain size rather than substantial differences in relative commissural investment. (C) Representative sagittal T2-weighted images allowing qualitative comparison of cerebellar morphology across species. Cerebellar foliation and overall cerebellar expansion vary markedly among taxa, with particularly elaborate folial patterns observed in penguins, toucans, and crows. (D) Representative cerebellar histological sections from selected species illustrating interspecific differences in folial branching and structural complexity. (E) Quantification of cerebellar folial branching. The number of basal branches (A) exhibits relatively limited interspecific variation, whereas the number of terminal branches (B) varies more extensively and is elevated in species with more highly elaborated cerebella. Together, these findings support a pattern of mosaic, region-specific diversification in avian brain organization.

the present analysis does not directly resolve functional specialization. Notably, penguins displayed pronounced cerebellar expansion despite having a relatively small AC, suggesting a dissociation between the elaboration of interhemispheric and sensorimotor systems. Together, these observations are consistent with mosaic, region-specific diversification of internal brain architecture rather than uniform scaling across all major brain divisions.

Template-Based 3D Morphometry and Mosaic Scaling

High-resolution MRI enables not only comparisons of overall brain morphology across species but also quantitative analyses of individual brain regions. Using the MRI datasets, we reconstructed three-dimensional (3D) brain models for 16 avian species and an Egyptian rousette bat, which was included as a flying mammalian outgroup. Representative renderings are shown from anterior-left (Fig. 3A, left) and posterior-right (Fig. 3A, right) perspectives. The quality and smoothness of the reconstructed 3D surfaces depended on the image acquisition resolution, with higher-resolution datasets producing more refined reconstructions. These renderings provide a clear visualization of the spatial relationships among major brain divisions, including the telencephalon, midbrain, and cerebellum, within each species.

We next established a template-based morphometric workflow to convert these anatomical reconstructions into comparable regional measurements (Fig. 3B). In this workflow, each brain was aligned to a species-specific template, major brain compartments were segmented, and the resulting parcellations were used to generate 3D surface models and segmentation-derived volume estimates. This procedure allowed the same major anatomical compartments to be compared across species despite substantial differences in brain size and overall morphology. To quantify regional investment, we performed volumetric segmentation using species-specific templates and calculated the relative volume fractions of the telencephalon, midbrain, and cerebellum (Fig. 3C). The resulting proportional volume profiles suggested that overall brain size alone may not fully capture interspecific variation in internal brain organization. Instead, individual species showed distinct combinations of relative telencephalic, midbrain, and cerebellar allocation. For example, species with prominent cerebellar morphology did not necessarily show parallel increases in all other major brain divisions, suggesting that regional compartments can vary semi-independently. These 3D volumetric data therefore extend the two-dimensional observations from T2-weighted sections and provide an exploratory quantitative framework for evaluating mosaic scaling across avian lineages. This standardized workflow provides a foundation for phylogenetically informed analyses of mosaic scaling across diverse avian lineages.

Histological Validation of MRI-Derived Boundaries

To assess the biological validity of the parcellation framework, we compared MRI-derived boundaries with complementary histological data from three representative species occupying distinct ecological and phylogenetic positions: the large-billed crow, gentoo penguin, and mandarin duck (Fig. 4). Across all three taxa, MRI-defined boundaries corresponded closely to histological transitions. Nissl staining confirmed that cytoarchitectonic changes aligned with the anatomical borders used for MRI segmentation, whereas Luxol Fast Blue (LFB) staining highlighted major white-matter compartments and long-range pathways identified by diffusion MRI. Together, these cross-modal correspondences provide tissue-level validation of the morphometric and diffusion-derived measurements and support the consistency of the parcellation framework across species.

Divergent Long-Range Wiring and Microstructural Profiles

Diffusion MRI tractography and fractional anisotropy (FA) mapping revealed both conserved and species-specific features of avian brain organization (Fig. 5). We first examined region-seeded tractography to compare large-scale trajectory patterns among representative species (Fig. 5A). To compare long-range trajectory patterns, we performed tractography from four brain regions, namely, the optic lobe, dorsal cortex, cerebellum, and anterior cortex, in three representative

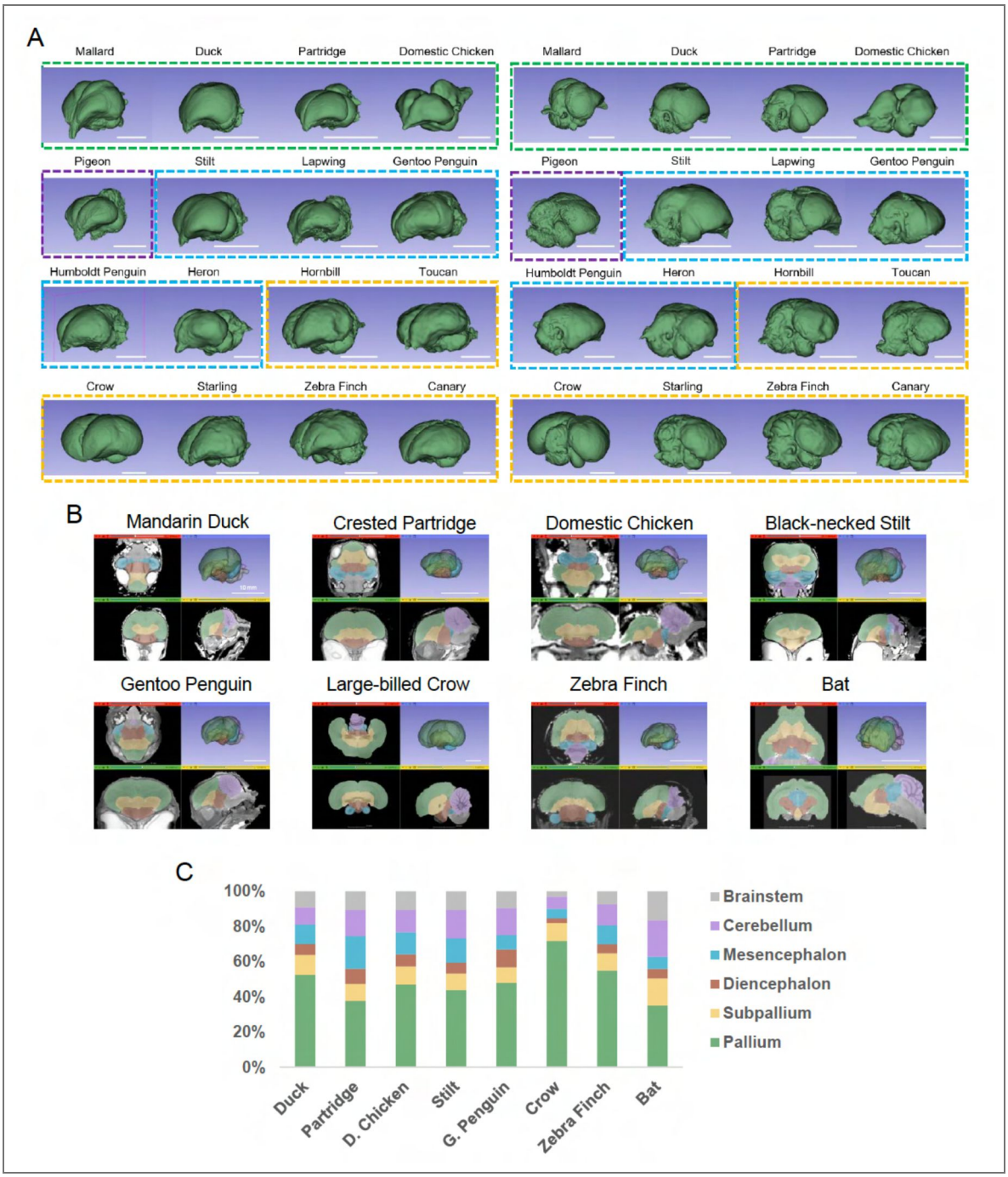

Figure 3. Template-based registration enables standardized 3D morphometry and mosaic scaling quantification.

(A) Three-dimensional (3D) reconstructions of brains from 16 avian species, rendered from anterior-left (left) and posterior-right (right) viewpoints. The fidelity of the reconstructed surfaces reflects image acquisition resolution, with higher-resolution datasets producing smoother and more detailed reconstructions. (B) Schematic overview of the morphometric workflow, including species-specific template construction, registration into a common comparative space, and template-guided segmentation of major brain compartments. Representative overlays demonstrate the correspondence between MRI data and segmented 3D reconstructions. (C) Volumetric quantification of major brain divisions based on segmentation-derived voxel counts, expressed as proportions of total brain volume to facilitate comparison of relative regional investment across species. This workflow enables standardized evaluation of mosaic scaling across diverse avian lineages.

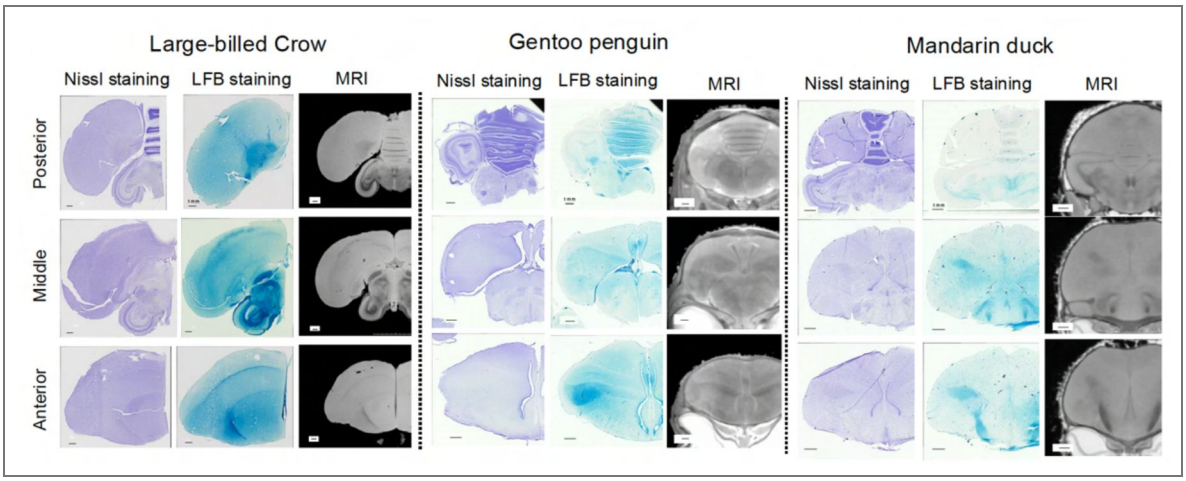

Figure 4. Histological validation links MRI-derived boundaries and diffusion-related measures to tissue architecture.

(Left) Representative Nissl-stained sections across selected taxa illustrating cytoarchitectonic transitions that align with major MRI-defined anatomical boundaries used for parcellation. (Middle) Luxol Fast Blue (LFB) staining highlights white-matter architecture and major fiber-rich compartments corresponding to MRI-defined white matter. Together, these histological observations support the cross-species consistency of the segmentation framework and provide tissue-level validation for the interpretation of MRI- and diffusion-derived metrics.

species: chick, gentoo penguin, and large-billed crow. We reconstructed approximately 1.0×10^7 streamlines and applied clustering analysis to identify the major trajectory groups. This analysis allowed us to compare how reconstructed trajectories associated with homologous or anatomically corresponding regions were distributed within each brain. The most pronounced interspecific differences were associated with optic-lobe tractography. In chick, reconstructed streamlines were largely restricted to the optic lobe, with only limited extension into lateral pallial territories. In contrast, optic-lobe-associated trajectories in the gentoo penguin were distributed more broadly throughout the brain. Pallial tractography also differed between species. In chick, dorsal-cortex-associated trajectories were dominated by dorsotemporal pathways and remained largely confined to pallial compartments. In the gentoo penguin, however, an additional distinct trajectory group was identified within a lateral temporal cortex-like subdivision. By comparison, cerebellum- and anterior-cortex-associated tractography showed broadly similar patterns in chick and the gentoo penguin, with many reconstructed trajectories remaining within their respective anatomical compartments. Thus, Fig. 5A indicates that some trajectory classes are broadly conserved across species, whereas optic-lobe- and pallium-associated trajectories show more conspicuous interspecific divergence. These findings indicate that tractography captures both conserved and region-specific patterns of organization across species.

We next examined whole-brain FA maps to compare regional microstructural organization independently of streamline trajectory distributions (Fig. 5B, Movie 1-4). Whole-brain FA mapping further revealed interspecific differences in microstructural organization. In the large-billed crow, reconstructed trajectories were relatively enriched in the anterior lobe, whereas FA values were comparatively elevated in the cerebellum and optic lobe. In the gentoo penguin, FA values were likewise elevated in the cerebellum, although this was not accompanied by a corresponding increase in relative trajectory abundance. Instead, reconstructed trajectories were enriched in the dorsal cortex. In the mammalian outgroup, the Egyptian rousette, reconstructed trajectories showed a close association between the optic and temporal lobes, together with relative enrichment within the dorsal cortex. These observations suggest that FA-based microstructural contrast and tractography-derived trajectory abundance capture partially distinct aspects of brain organization. To summarize these relationships quantitatively, we compared regional values derived from reconstructed trajectories and FA maps across representative species (Fig. 5C). The tractography-derived summary highlighted species-specific differences in the relative distribution of reconstructed trajectories, whereas the FA-based summary emphasized regional variation in tissue anisotropy. The partial mismatch between these two measures was particularly evident in the gentoo penguin, in which cerebellar FA was elevated despite the absence of a corresponding enrichment of cerebellar trajectories. This dissociation indicates that regional microstructural specialization does not necessarily scale directly with the number or distribution of reconstructed streamlines.

Collectively, the tractography and FA analyses indicate that avian species share broad features of large-scale brain organization while exhibiting substantial differences in long-range trajectory distributions and regional microstructural profiles.

Discussion

A Unified Framework for Comparative Avian Neuroanatomy

Our study establishes a standardized MRI-based framework for quantifying internal brain organization across 16 avian species occupying diverse ecological niches. Previous comparative studies of avian brain evolution have relied primarily on measures of overall brain size, endocast morphology, or neuron-number scaling (3, 18–20). Although these approaches have yielded valuable insights, they cannot directly resolve internal anatomical organization or long-range pathway architecture. By integrating curated datasets from the ABC (13) with publicly available MRI resources, we provide a scalable and transferable platform for comparative neuroanatomy that can be extended to other vertebrate groups wherever structural and diffusion MRI data are

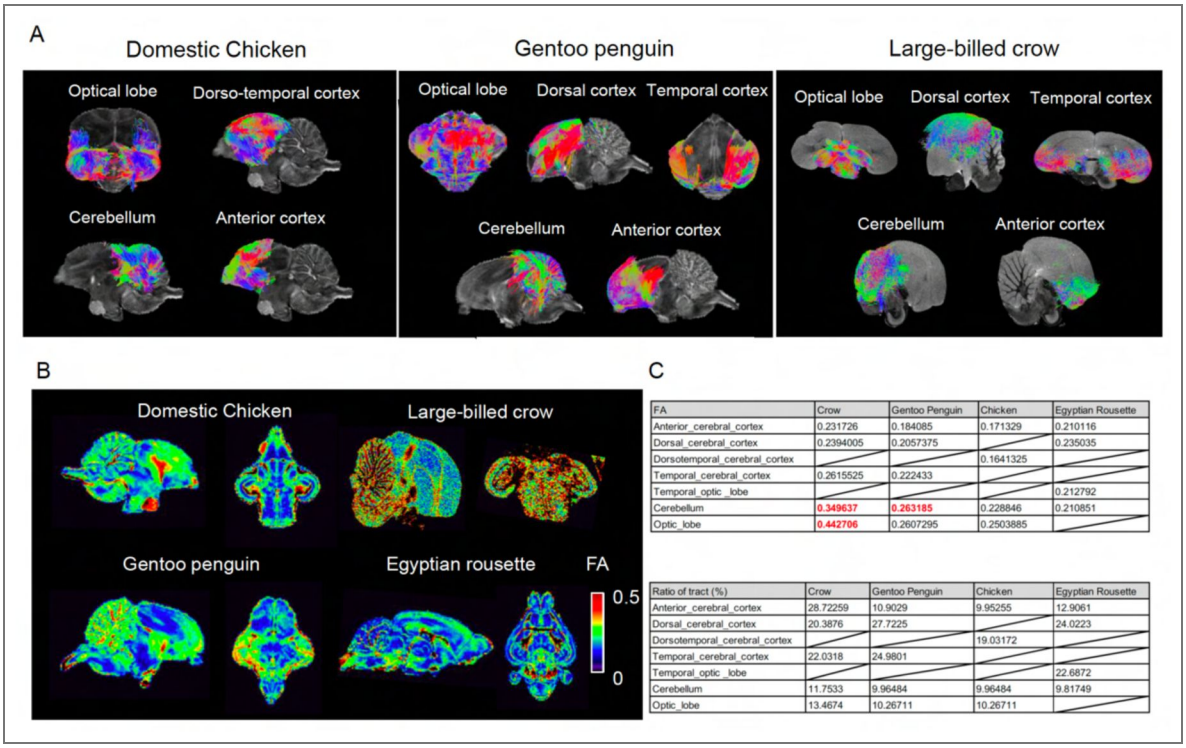

Figure 5. Diffusion MRI tractography and anisotropy mapping reveal conserved and divergent long-range organization across species.

(A) Region-seeded diffusion MRI tractography in chick, gentoo penguin, and large-billed crow. Streamlines were generated from four regions of interest (ROIs)—the optic lobe, dorsal cortex, cerebellum, and anterior/temporal cortex—and subsequently clustered to identify the major trajectory groups. (B) Whole-brain fractional anisotropy (FA) maps from representative species illustrating interspecific differences in regional microstructural organization. (C) Quantitative comparison of tractography- and FA-derived regional metrics in chick, gentoo penguin, and Egyptian rousette bat. The upper and lower tables summarize relative regional distributions derived from reconstructed trajectories and FA values, respectively. Together, these analyses indicate that species share broad organizational features while differing substantially in inferred long-range routing patterns and regional microstructural profiles.

available at the species level (21, 22). More broadly, this framework facilitates a shift from global brain-size correlations toward region-specific, phylogenetically informed hypotheses of neural diversification (18, 23).

Mosaic Evolution and Ecological Diversification of Avian Brains

Our findings strongly support a mosaic model of avian brain evolution, in which individual brain divisions vary semi-independently rather than scaling uniformly as part of a single integrated structure (19). This interpretation extends previous work linking ecological variation to overall brain size by suggesting that ecological pressures are also reflected in the allocation of neural investment among internal brain regions (23–27). Under this framework, species facing distinct ecological challenges, such as rapid maneuvering, long-distance navigation, or underwater foraging, exhibit differential investment in sensory and sensorimotor systems, accompanied by corresponding changes in long-range white-matter organization (23, 28, 29).

Several observations from our dataset illustrate this pattern. The pronounced cerebellar expansion observed in the gentoo penguin, together with elevated FA within cerebellar white matter, is consistent with enhanced sensorimotor specialization associated with aquatic locomotion. By contrast, the AC exhibited conspicuous qualitative variation across species and appeared particularly prominent in large-billed crow, starling, and canary. However, because AC area scaled approximately with overall brain size in the present analysis, these observations should be interpreted with caution. Rather than providing evidence for lineage-specific expansion of commissural investment, they identify interhemispheric architecture as a potentially important axis of avian forebrain diversification that warrants further investigation using residual-based allometric approaches, broader taxonomic sampling, and tract-level analyses (23, 30).

More generally, variation in pallial and subpallial investment, cerebellar allocation, and the balance between commissural and association-type wiring patterns may represent complementary neural solutions to habitat-specific control demands that evolve semi-independently across avian lineages (18, 19). Brain evolution has traditionally been framed in terms of two major models, concerted evolution and mosaic evolution. An important unresolved question is when mosaic divergence emerges during development. Recent work in axolotl suggests that these mechanisms are not mutually exclusive but may jointly contribute to brain development and evolutionary diversification (31). Consistent with this possibility, post-hatching changes in avian brain morphology have been documented, and comparative studies indicate that sensory specializations, most notably in the olfactory bulbs and more broadly throughout major visual pathways including the optic tectum, are associated with ecological diversification in birds (5, 7, 32). Taken together, these findings raise the possibility that post-hatching brain development is further shaped in a species-specific manner by the ecological and behavioral demands experienced by individual lineages.

Long-Range Wiring as a Dimension of Brain Diversification

Diffusion MRI tractography further suggests that long-range wiring organization represents a major axis of interspecific variation (22). In particular, the contrast between the relatively localized optic-lobe-associated trajectories observed in chick and the more broadly distributed trajectories observed in the gentoo penguin indicates that sensory routing architectures can differ substantially among species. The presence of a distinct lateral temporal cortex-like trajectory pattern in the penguin further supports the idea that ecological specialization may be accompanied by reorganization of pallial connectivity motifs.

At the same time, tractography-derived trajectory distributions and diffusion-based microstructural indices provided partially independent information, consistent with the broader observation that tractography and scalar diffusion metrics capture different aspects of tissue organization (22, 33, 34). For example, elevated cerebellar FA in the gentoo penguin was not accompanied by increased streamline representation within the same region, whereas dorsal pallium-associated trajectories were comparatively prominent. Inthe large-billed crow, by contrast, elevated FA was most evident in the cerebellum and optic lobe, whereas trajectory

enrichment was concentrated in the anterior lobe. These comparisons underscore the complementary nature of tractography-derived trajectory distributions and diffusion-based microstructural measures and highlight the importance of interpreting both jointly in comparative analyses (22, 33).

Histological Anchoring and Developmental Implications

A major strength of the present framework is that MRI-derived measurements were anchored to histological features. Nissl staining supported the anatomical boundaries identified by MRI, whereas myelin staining corresponded closely to major white-matter compartments and principal diffusion-derived pathways. This histological validation strengthens the biological interpretation of MRI-based volumetric and diffusion measurements and provides a foundation for identifying tissue properties that may contribute to interspecific variation in diffusion metrics, including myelination, axon caliber, axonal packing density, and orientation dispersion (22, 33). More broadly, linking MRI-derived phenotypes to underlying tissue properties creates new opportunities to connect comparative neuroanatomy with the developmental mechanisms that shape regional brain architecture (35, 36).

A Case Study of Mosaic Specialization: The Penguin Brain

Penguins provide a particularly informative example of mosaic neuroanatomical specialization. In our dataset, the gentoo penguin exhibited a distinctive combination of relatively reduced AC prominence and pronounced cerebellar expansion, consistent with lineage-specific reallocation of neural investment. In birds, telencephalic interhemispheric connectivity relies on a limited number of commissural pathways, with the AC serving as the principal forebrain commissure. Tract-tracing studies have shown that AC projections originate from restricted arcopallial and amygdaloid sources and project broadly to contralateral sensorimotor and limbic targets, suggesting that variation in AC prominence may reflect differences in commissural routing rather than serving as a simple indicator of any particular sensory modality (17). These studies further indicate that, unlike in mammals, interhemispheric transfer of olfactory information in birds is not mediated primarily through the AC but may instead involve alternative diencephalic pathways such as the habenular commissure (17).

Accordingly, the reduced AC prominence observed in penguins should not be interpreted directly as evidence of olfactory specialization. Rather, it may reflect lineage-specific reorganization of commissural architecture associated with differences in the integration of bilateral sensory information across hemispheres. However, the present data do not allow us to distinguish among several non-mutually exclusive explanations, including altered reliance on non-AC commissural pathways, changes in interhemispheric sensory integration, or a greater emphasis on rapid unilateral processing.

The marked cerebellar expansion observed in penguins is likewise consistent with increased demands on visuovestibular integration, gaze stabilization, and precise sensorimotor timing. Although these characteristics are compatible with the requirements of three-dimensional underwater locomotion, they may not be unique to aquatic specialization and could instead reflect more general adaptations associated with high locomotor performance in birds. Together, these findings suggest that penguin brain evolution involved coordinated yet regionally selective reorganization of commissural and sensorimotor systems. The ecological and functional significance of these changes, however, remains to be evaluated through broader comparative analyses.

Limitations and Future Directions

Several limitations should be considered when interpreting the present findings. Cross-species MRI comparisons remain influenced by variation in acquisition conditions, and diffusion tractography provides an indirect reconstruction of pathway organization rather than direct

evidence of axonal connectivity (22). In addition, broader taxonomic sampling will be required to disentangle correlated ecological variables and determine whether the observed patterns reflect general principles of avian brain organization or lineage-specific specializations (18, 23).

For example, the penguin data suggest a distinctive combination of cerebellar organization, tectal projection patterns, and pallial trajectory architecture. However, additional sampling of both aquatic and nonaquatic species will be necessary to determine the extent to which these features are characteristic of aquatic adaptation more broadly. Despite these limitations, the present framework provides standardized measures of internal anatomical organization, quantitative volumetry, and whole-brain connectivity in a format suitable for comparative analyses. As such, it enables avian neuroanatomy to move beyond coarse comparisons of brain size toward explicit, testable hypotheses linking ecological demands, developmental programs, and internal circuit organization (36).

Conclusion

We present a harmonized avian MRI resource together with a reproducible analytical framework for quantifying internal brain organization across diverse ecological contexts. By revealing mosaic variation in regional investment and long-range wiring architecture, while anchoring MRI-derived metrics to histological features, this study provides a scalable foundation for linking avian neuroanatomical diversity to ecological pressures, developmental programs, and evolutionary trajectories.

Materials and Methods

Brain Samples

We assembled a comparative MRI dataset comprising 16 avian species representing major avian clades and diverse ecological and behavioral categories, together with a flying mammalian outgroup, the Egyptian rousette bat, for selected diffusion-based comparisons. MRI datasets were obtained from two sources: (i) previously deposited datasets from the ABC and (ii) publicly available avian MRI datasets for canary, starling, pigeon, and zebra finch. Datasets were included when T2-weighted structural images provided sufficient contrast to delineate major brain compartments and, for diffusion analyses, when diffusion-weighted images possessed adequate angular and spatial resolution for tensor reconstruction and deterministic tractography. For publicly available datasets, original acquisition metadata were retained and integrated into a standardized metadata table.

Image Preprocessing and Template Construction

Before analysis, T2-weighted images were inspected for orientation, field-of-view coverage, and major imaging artifacts. Non-brain tissue was removed manually or semi-automatically using 3D Slicer, after which brains were reoriented into a common anatomical convention based on corresponding coronal, sagittal, and horizontal planes. When required, image intensity was adjusted solely for visualization and identification of anatomical boundaries; all quantitative segmentations were performed using the original structural image volumes. Species-specific templates were generated from the available structural images for each species and used as reference spaces for regional parcellation. For cross-species visualization, segmented regions were exported as 3D surface models and rendered from standardized viewpoints. Manual reorientation was performed in 3D Slicer (version 5.8.1) using the Transforms module, with the anterior commissure and midsagittal plane used as anatomical landmarks. Only rigid linear transformations, consisting of translations and rotations, were applied.

Anatomical Segmentation and Volumetric Analysis

T2-weighted images were imported into 3D Slicer, and anatomical segmentation was performed using the Segment Editor module. First, multiple consecutive slices were coarsely labeled with the Paint tool to distinguish the whole brain (“brain”) from surrounding non-brain tissue (“other”).

The whole brain was then extracted as a single segment using the Grow from Seeds algorithm. For regional parcellation, anatomical boundaries were delineated and filled using the Draw tool on every other slice, and intermediate slices were generated by interpolation with Fill between Slices to produce 3D segmentations. Segment volumes were calculated using the Segment Statistics module. Volumes (mm^3) were derived from the number of voxels contained within each segment, and the proportional volume of each region was expressed relative to total brain volume.

Anterior Commissure (AC) Measurement

The AC was identified on coronal T2-weighted sections as a transverse commissural fiber bundle located ventral to the telencephalic midline within the rostral forebrain/preoptic region. For each species, AC area was measured on the coronal section exhibiting the largest cross-sectional profile of the commissure. The AC was manually outlined as a region of interest, and the corresponding whole-brain cross-sectional area was measured on the same section. Relative AC size was calculated as the ratio of AC area to whole-brain area. Allometric relationships were evaluated by comparing AC area with whole-brain area across species. For each species, AC area and whole-brain cross-sectional area were measured once on a single coronal section corresponding to the maximal cross-sectional profile of the AC.

Cerebellar Foliation Analysis

Cerebellar foliation was assessed using midsagittal or near-midsagittal T2-weighted sections and, when available, corresponding histological sections. The primary cerebellar arbor was traced from the central white-matter core, and folial branches were categorized as either basal or terminal branches. Basal branches were defined as primary branches arising from the central cerebellar white-matter trunk, whereas terminal branches were defined as distal folial endings visible at the pial surface. Branch numbers were quantified from equivalent anatomical planes across species whenever possible. Among the 14 bird species examined, cerebellar foliation was analyzed primarily using midsagittal T2-weighted images. The Humboldt penguin was excluded because the cerebellar folial architecture could not be reliably identified in the available MRI data. For the domestic chicken, branch counts were performed using an existing chicken brain atlas, as suitable midsagittal MRI sections were not available. All counts were performed by a single observer.

Histological Validation

To validate MRI-derived anatomical boundaries, histological analyses were performed in three representative species: the large-billed crow, gentoo penguin, and mandarin duck. Brains were sectioned in planes corresponding to the MRI images and stained using Nissl staining to visualize cytoarchitecture and Luxol fast blue (LFB) staining to identify myelinated fiber-rich compartments.

Histological sections were prepared at a thickness of 50–100 μm. Before Nissl and LFB staining, sections were defatted. Briefly, sections were immersed twice in distilled water for 2 min each and then in 70% ethanol for 2 min. Sections were subsequently immersed in 100% ethanol five times for 2 min each, followed by xylene for 5 min. After defatting, sections were rehydrated through four changes of 100% ethanol for 2 min each and then processed for either LFB or Nissl staining.

For LFB staining, defatted slides were immersed in 95% ethanol for 1 min. Luxol fast blue was dissolved in 95% ethanol at a final concentration of 0.2%, and the slides were incubated in this solution at 60°C for 16–24 h. After the staining solution had cooled to room temperature, the slides were removed and immersed in 95% ethanol for 2 min. The slides were then rinsed under running tap water and immersed in distilled water for 5 min. Differentiation was performed by gently agitating the slides in 0.05% lithium carbonate for 5–15 s, followed by agitation in 70% ethanol for 2 min. The slides were further differentiated in fresh 70% ethanol twice for 1 min each. After differentiation, the slides were washed under running tap water, immersed in distilled water for 5 min, dehydrated, cleared, and mounted.

For Nissl staining, defatted slides were immersed in 70% ethanol for 2 min, rinsed under running tap water, and immersed in distilled water for 5 min. The slides were then stained in 0.5% cresyl violet acetate for 6 min. Differentiation was performed by dipping the slides twice in 70% ethanol containing 0.1% acetic acid, followed by three dips in 95% ethanol containing 0.1% acetic acid. The solution was then replaced, and the slides were dipped three additional times in fresh 95% ethanol containing 0.1% acetic acid. The slides were subsequently dipped 10 times in 100% ethanol and transferred to fresh 100% ethanol for 2 min before dehydration, clearing, and mounting.

For dehydration and clearing, stained slides were immersed in 100% ethanol for 2 min and then cleared in xylene three times for 5 min each. Sections were mounted using a xylene-based mounting medium. Sections used for analysis were selected based on anatomical landmarks of the cerebrum and midbrain. Images were acquired using a Keyence BZ-X800 microscope.

MRI and histological sections were compared at anterior, middle, and posterior levels. Anatomical boundaries were evaluated based on the correspondence between MRI contrast, cytoarchitectonic transitions, and myelin-rich compartments.

Diffusion/Tractography Analysis

Diffusion-weighted images were reconstructed using the DTI model implemented in DSI Studio (*https://dsi-studio.labsolver.org/*). Diffusion tensors were estimated for each voxel, and scalar diffusion metrics, including FA, were derived from the resulting tensor model. Tractography was performed using the generalized deterministic tracking algorithm implemented in DSI Studio. For whole-brain tractography, 10,000,000 streamlines were generated using an FA threshold of 0.1, a minimum streamline length of 1 mm, and a maximum streamline length of 300 mm. Random maximum angle and trilinear interpolation settings were applied as global tracking parameters. The resulting streamlines were subsequently classified into ten clusters using the K-means clustering algorithm as implemented in DSI Studio.

Statistical Analysis

Morphometric and diffusion-derived measurements were analyzed as exploratory cross-species comparisons. AC cross-sectional area was compared with whole-brain cross-sectional area to evaluate broad allometric scaling across species, and relative AC size was calculated as the ratio of AC area to whole-brain cross-sectional area. Cerebellar foliation was quantified by counting basal and terminal branches from comparable midsagittal or near-midsagittal sections. Segmentation-derived regional volumes were normalized to total brain volume and expressed as proportional volume fractions. Diffusion-derived metrics, including streamline distributions and FA values, were compared across representative species to identify conserved and divergent anatomical patterns. Because the sample size and data sources varied across species, these analyses were treated as descriptive and hypothesis-generating rather than formal phylogenetically corrected tests.

Supplementary Figures

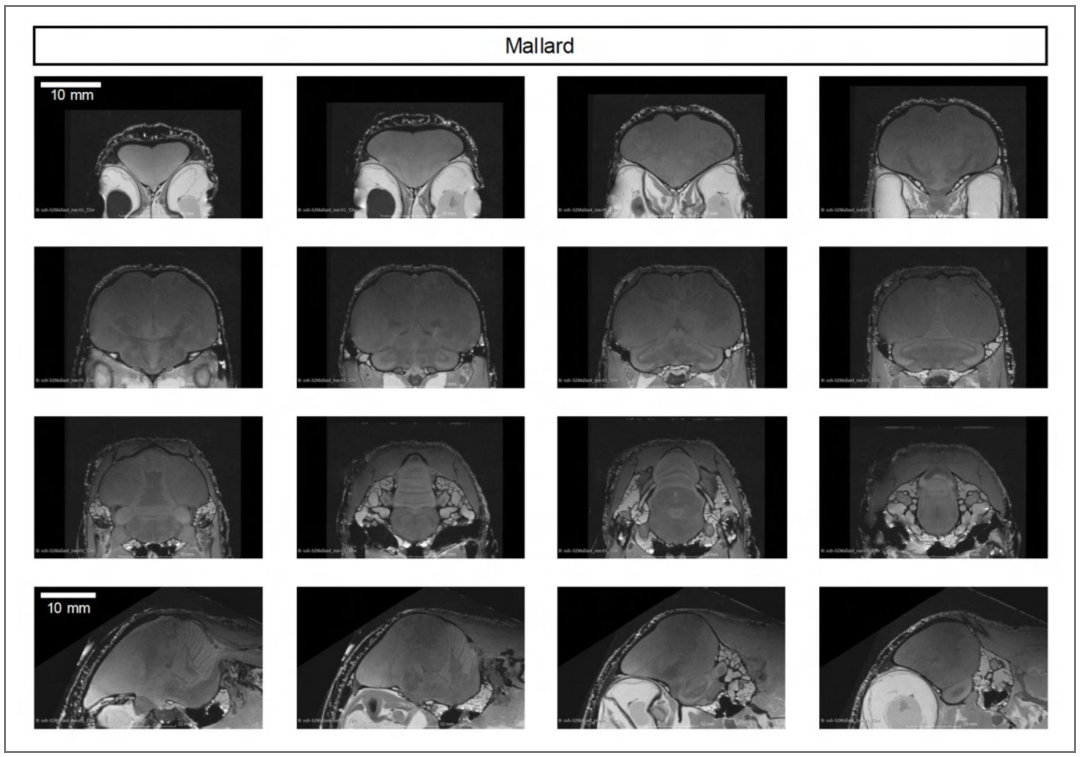

Fig. S1. Serial coronal and sagittal T2-weighted MRI sections of the mallard. Representative serial T2-weighted MRI sections of the mallard brain are shown to provide an overview of whole-brain morphology. Consecutive coronal sections are shown together with sagittal sections to illustrate the anatomical continuity of the forebrain, midbrain, cerebellum, and brainstem. Scale bars, 10 mm.

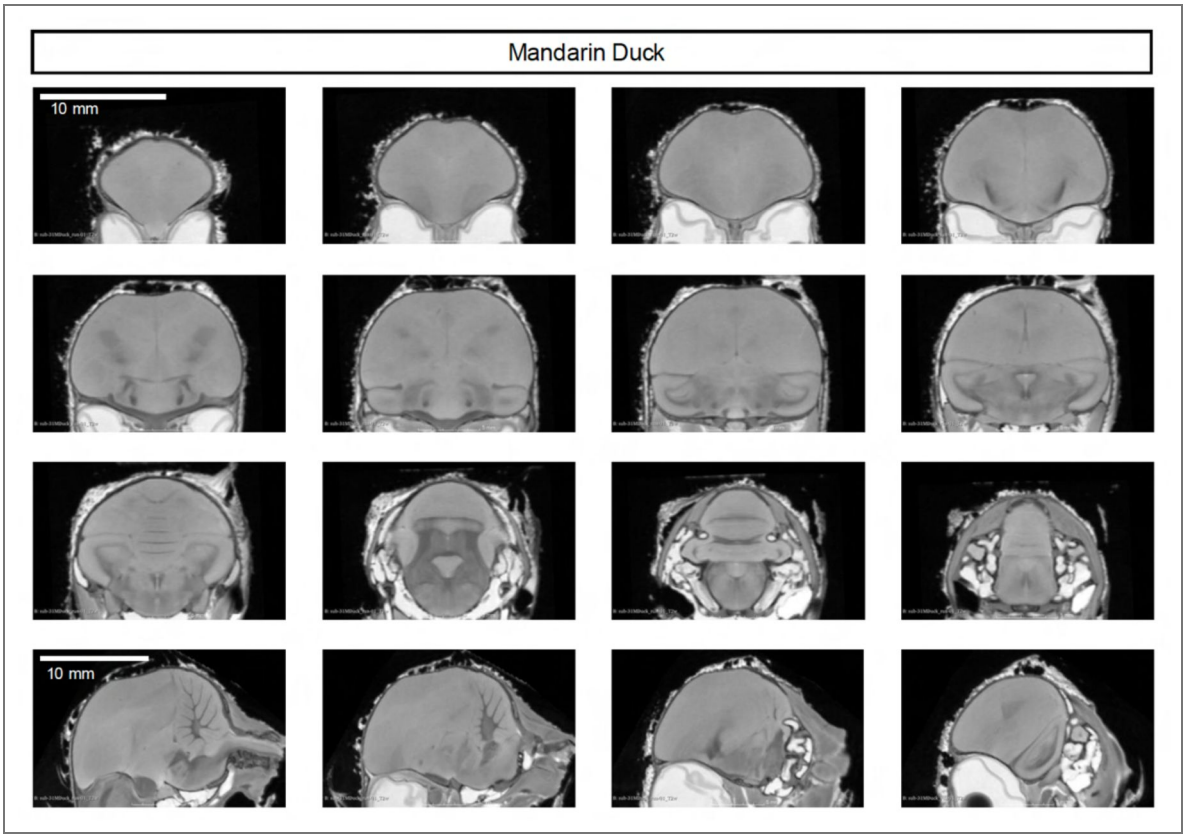

Fig. S2. Serial coronal and sagittal T2-weighted MRI sections of the mandarin duck.

Representative serial T2-weighted MRI sections of the mandarin duck brain are shown to provide an overview of whole-brain morphology. Consecutive coronal sections are shown together with sagittal sections to illustrate the anatomical continuity of the forebrain, midbrain, cerebellum, and brainstem. Scale bars, 10 mm.

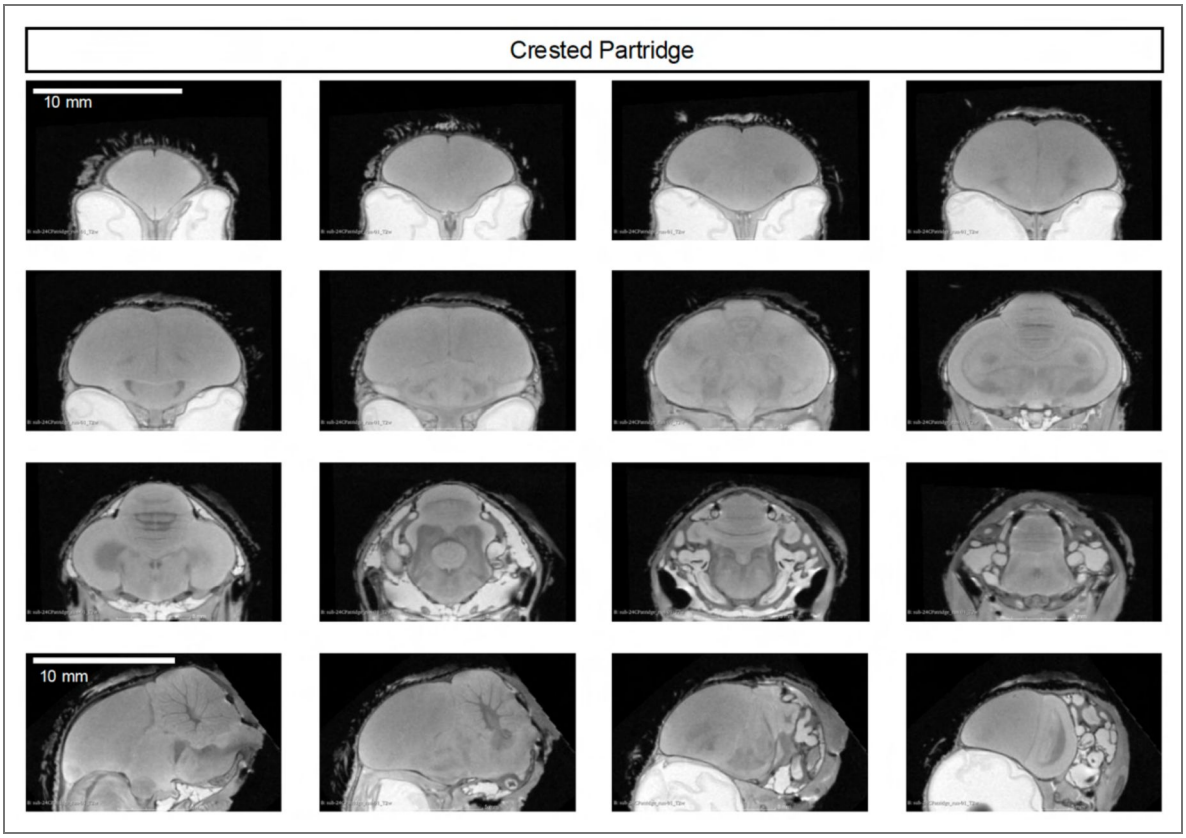

Fig. S3. Serial coronal and sagittal T2-weighted MRI sections of the crested partridge.

Representative serial T2-weighted MRI sections of the crested partridge brain are shown to provide an overview of whole-brain morphology. Consecutive coronal sections are shown together with sagittal sections to illustrate the anatomical continuity of the forebrain, midbrain, cerebellum, and brainstem. Scale bars, 10 mm.

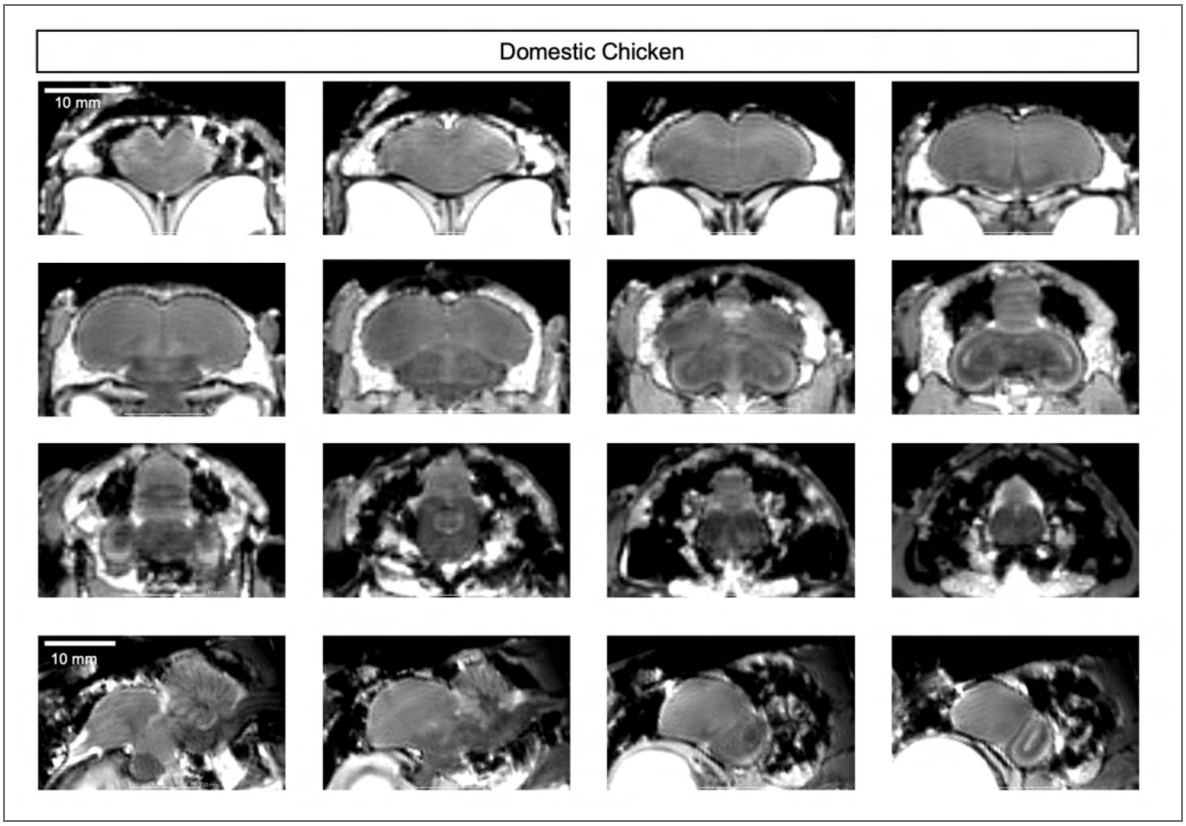

Fig. S4. Serial coronal and sagittal T2-weighted MRI sections of the domestic chicken.

Representative serial T2-weighted MRI sections of the domestic chicken brain are shown to provide an overview of whole-brain morphology. Consecutive coronal sections are shown together with sagittal sections to illustrate the anatomical continuity of the forebrain, midbrain, cerebellum, and brainstem. Scale bars, 10 mm.

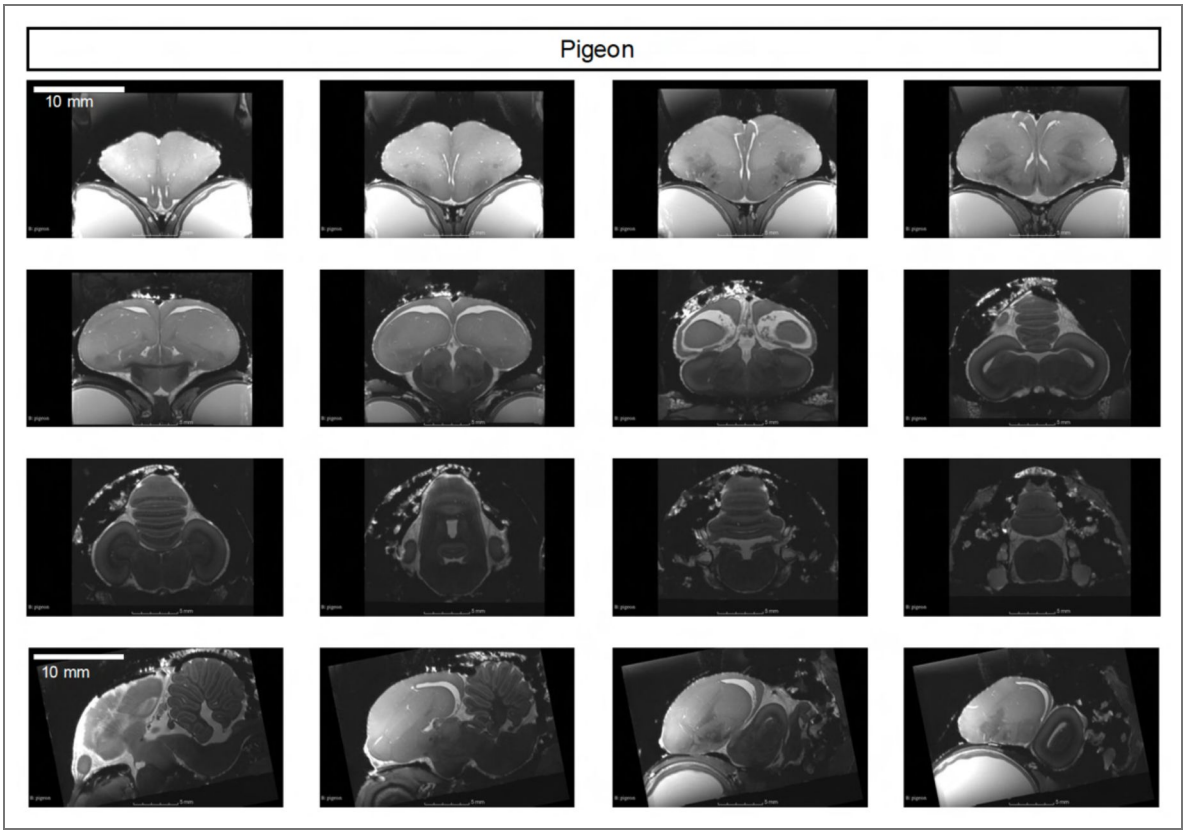

Fig. S5. Serial coronal and sagittal T2-weighted MRI sections of the pigeon.

Representative serial T2-weighted MRI sections of the pigeon brain are shown to provide an overview of whole-brain morphology. Consecutive coronal sections are shown together with sagittal sections to illustrate the anatomical continuity of the forebrain, midbrain, cerebellum, and brainstem. Scale bars, 10 mm.

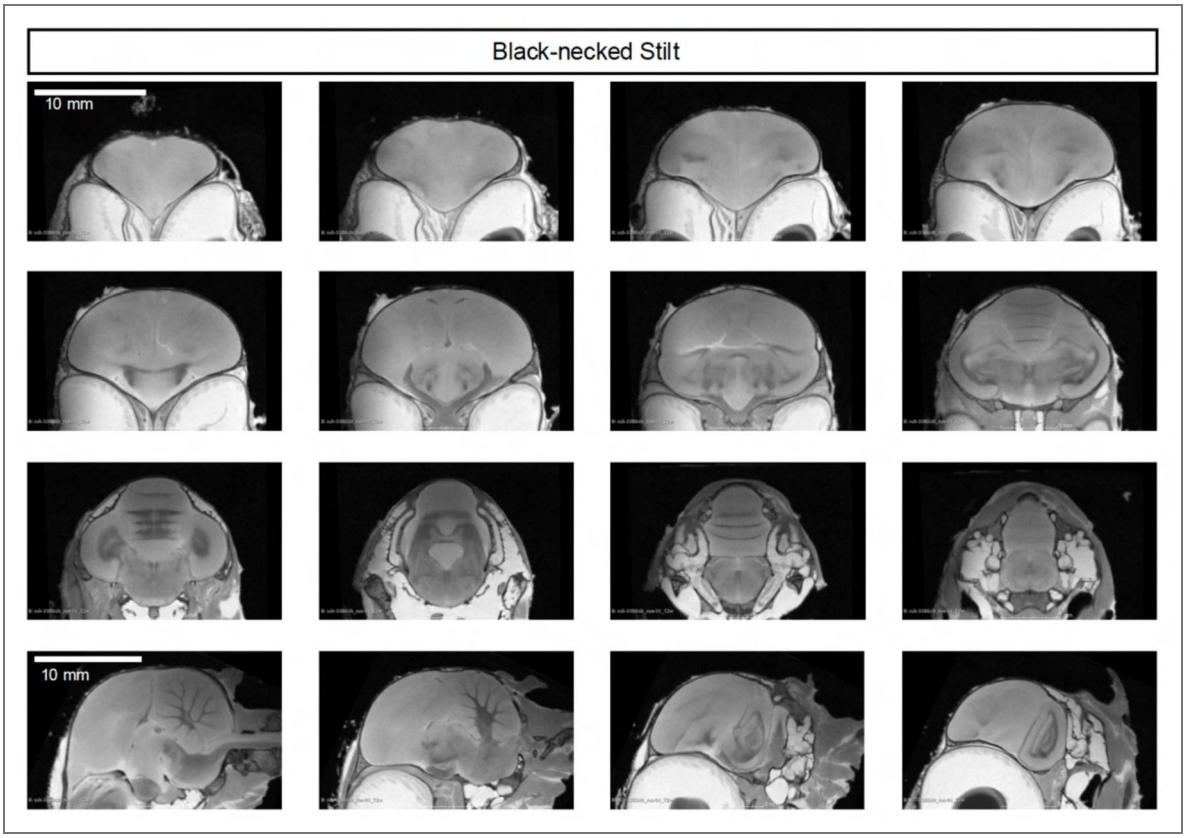

Fig. S6. Serial coronal and sagittal T2-weighted MRI sections of the black-necked stilt.

Representative serial T2-weighted MRI sections of the black-necked stilt brain are shown to provide an overview of whole-brain morphology. Consecutive coronal sections are shown together with sagittal sections to illustrate the anatomical continuity of the forebrain, midbrain, cerebellum, and brainstem. Scale bars, 10 mm.

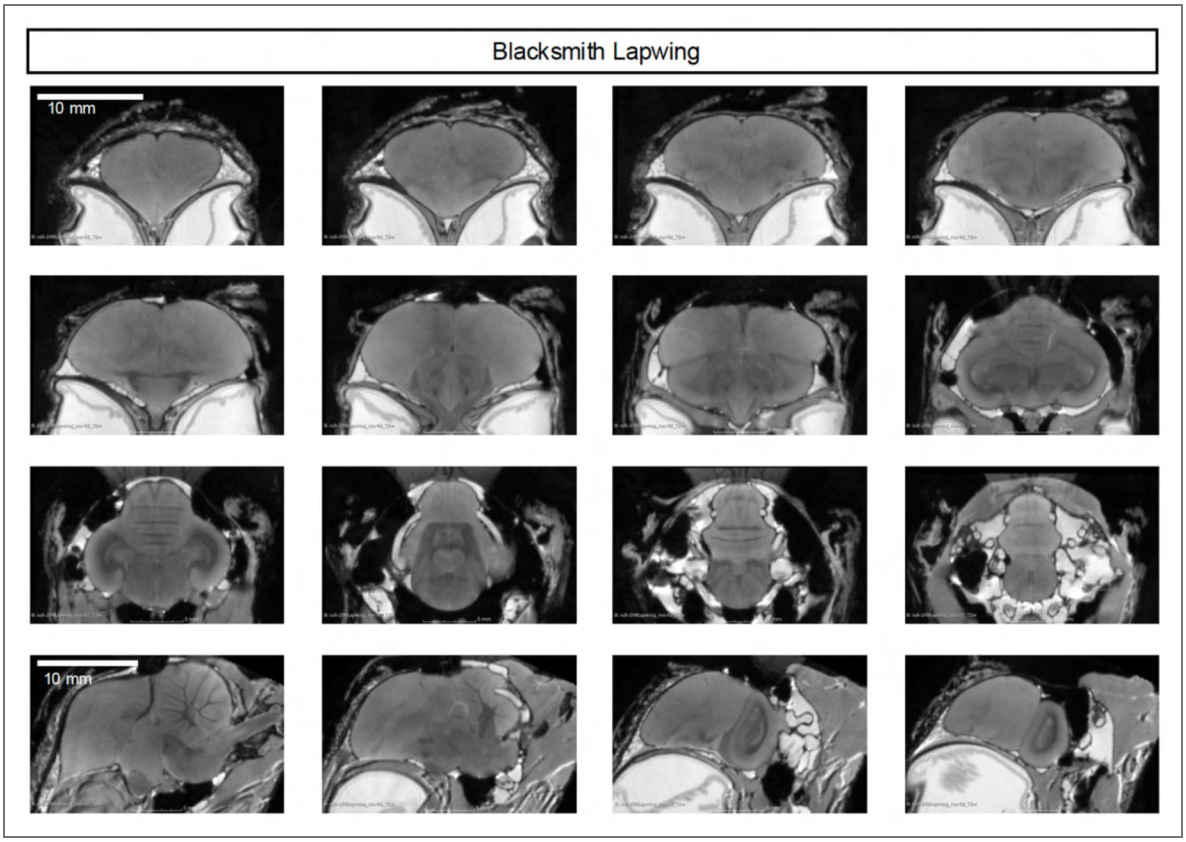

Fig. S7. Serial coronal and sagittal T2-weighted MRI sections of the blacksmith lapwing.

Representative serial T2-weighted MRI sections of the blacksmith lapwing brain are shown to provide an overview of whole-brain morphology. Consecutive coronal sections are shown together with sagittal sections to illustrate the anatomical continuity of the forebrain, midbrain, cerebellum, and brainstem. Scale bars, 10 mm.

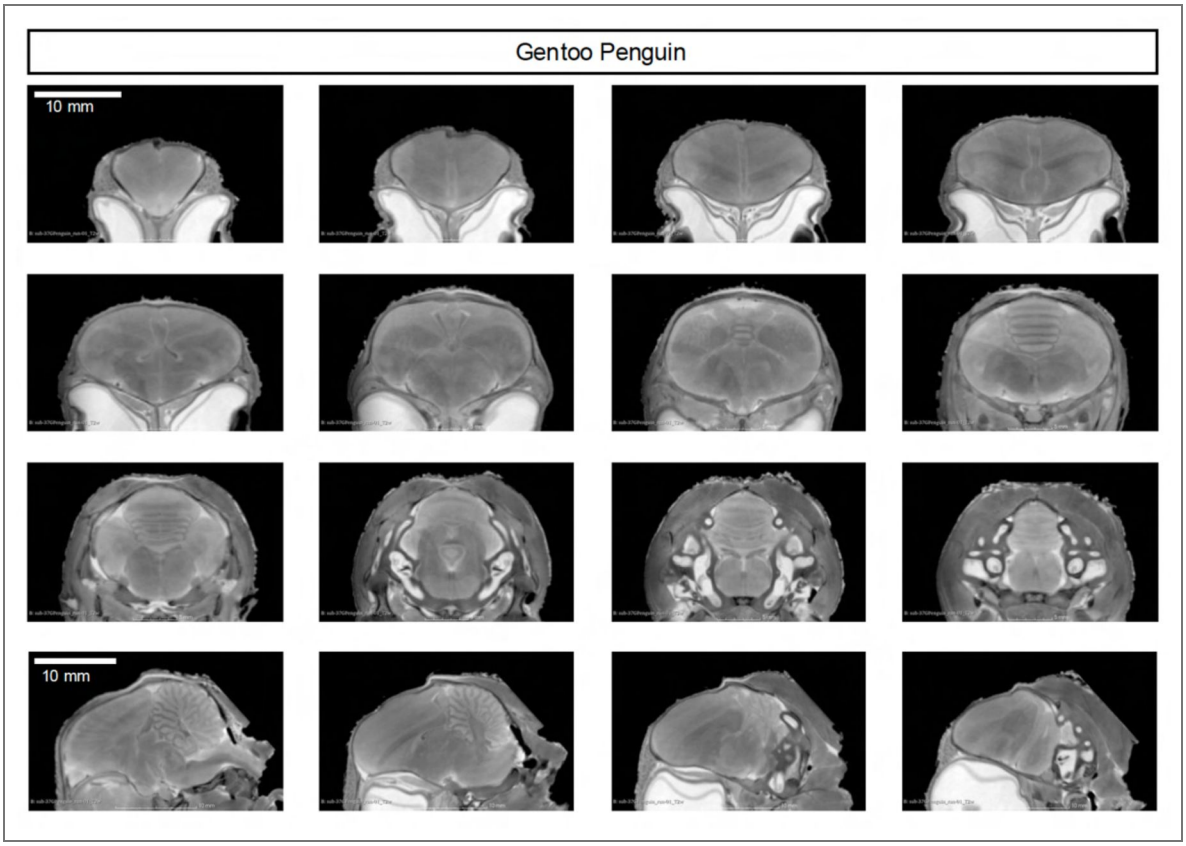

Fig. S8. Serial coronal and sagittal T2-weighted MRI sections of the gentoo penguin.

Representative serial T2-weighted MRI sections of the gentoo penguin brain are shown to provide an overview of whole-brain morphology. Consecutive coronal sections are shown together with sagittal sections to illustrate the anatomical continuity of the forebrain, midbrain, cerebellum, and brainstem. Scale bars, 10 mm.

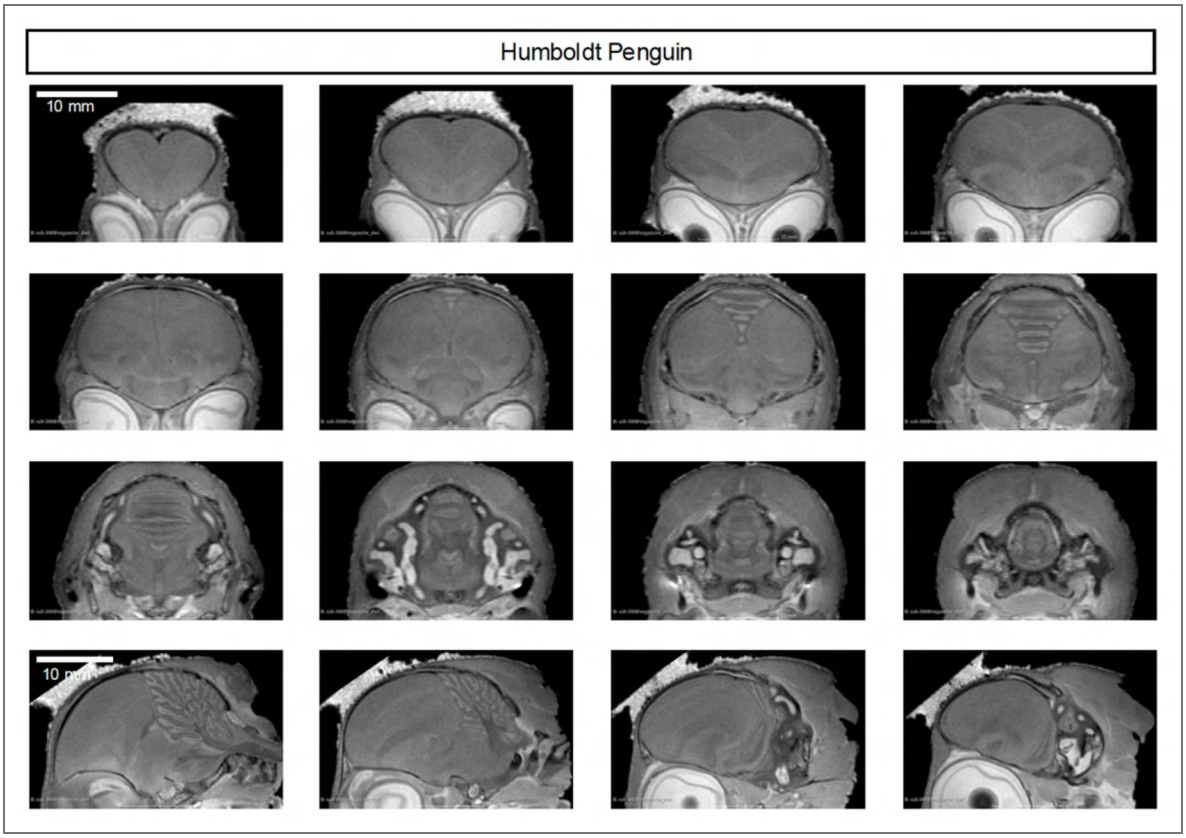

Fig. S9. Serial coronal and sagittal T2-weighted MRI sections of the Humboldt penguin.

Representative serial T2-weighted MRI sections of the Humboldt penguin brain are shown to provide an overview of whole-brain morphology. Consecutive coronal sections are shown together with sagittal sections to illustrate the anatomical continuity of the forebrain, midbrain, cerebellum, and brainstem. Scale bars, 10 mm.

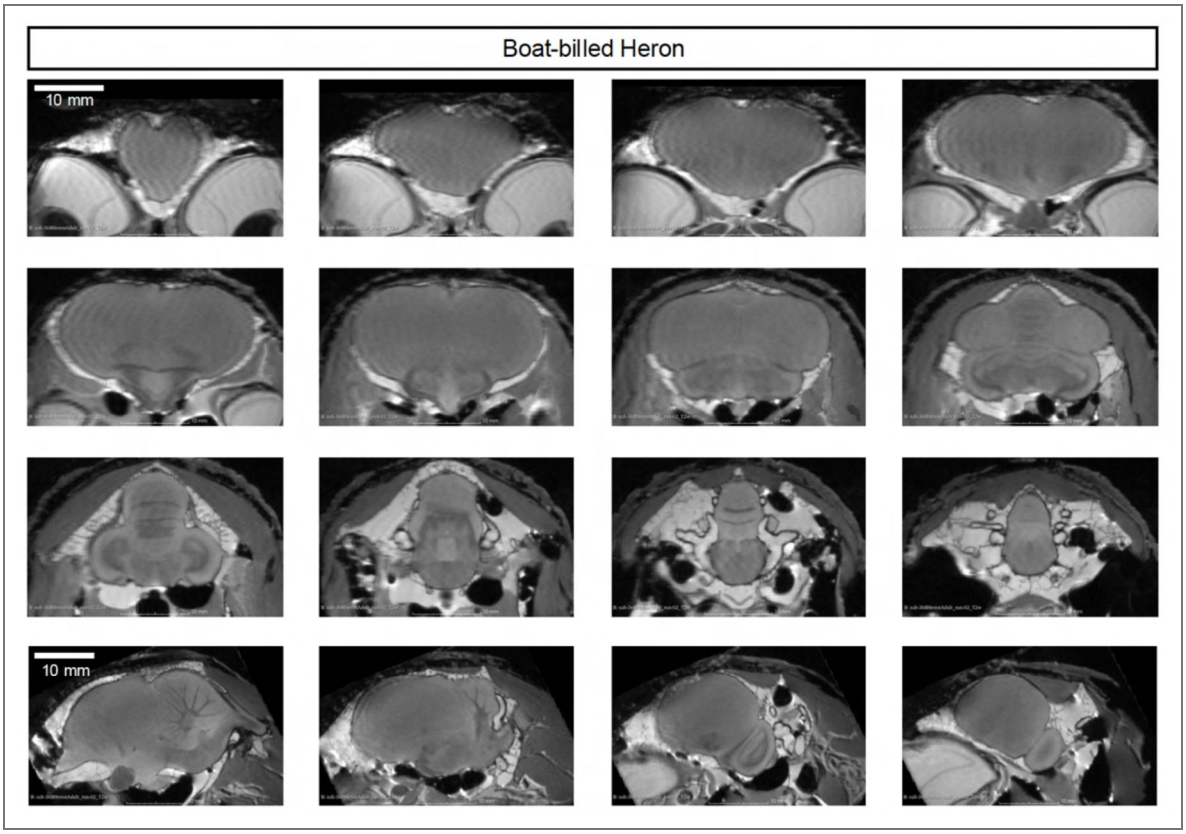

Fig. S10. Serial coronal and sagittal T2-weighted MRI sections of the boat-billed heron.

Representative serial T2-weighted MRI sections of the boat-billed heron brain are shown to provide an overview of whole-brain morphology. Consecutive coronal sections are shown together with sagittal sections to illustrate the anatomical continuity of the forebrain, midbrain, cerebellum, and brainstem. Scale bars, 10 mm.

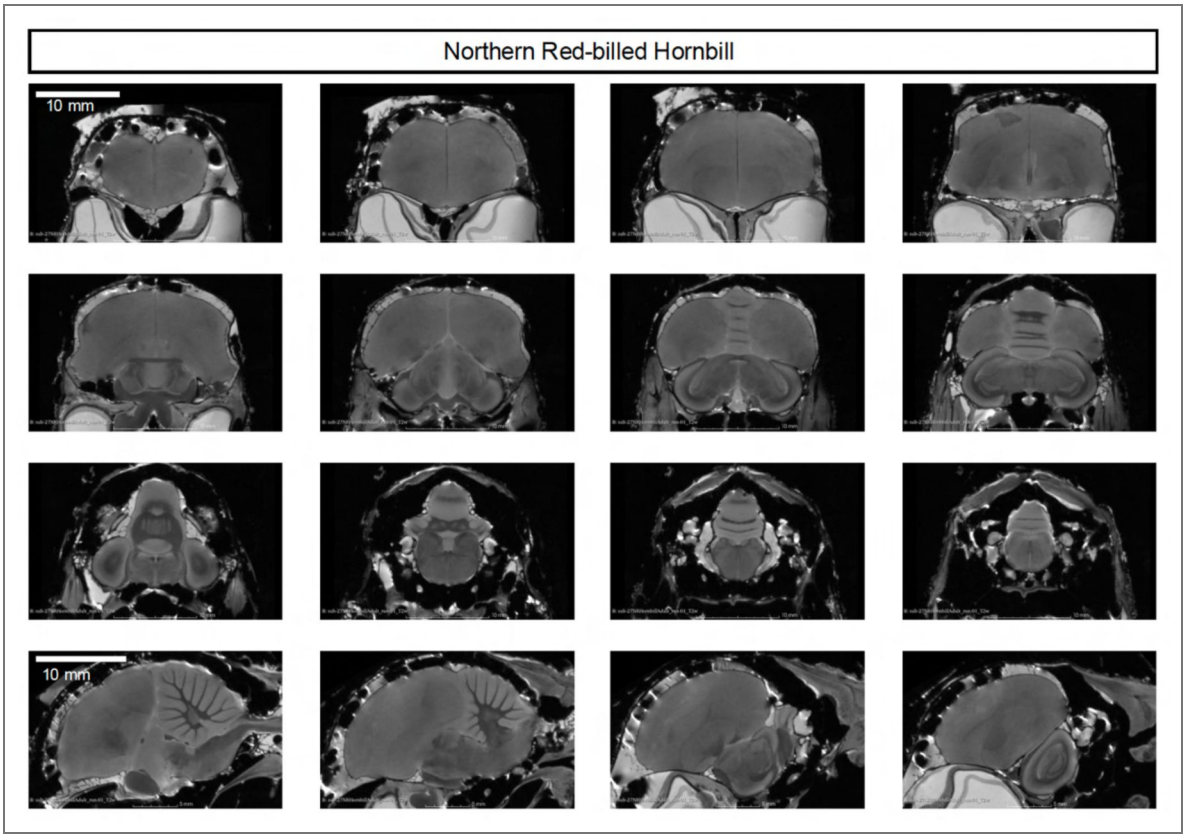

Fig. S11. Serial coronal and sagittal T2-weighted MRI sections of the northern red-billed hornbill.

Representative serial T2-weighted MRI sections of the northern red-billed hornbill brain are shown to provide an overview of whole-brain morphology. Consecutive coronal sections are shown together with sagittal sections to illustrate the anatomical continuity of the forebrain, midbrain, cerebellum, and brainstem. Scale bars, 10 mm.

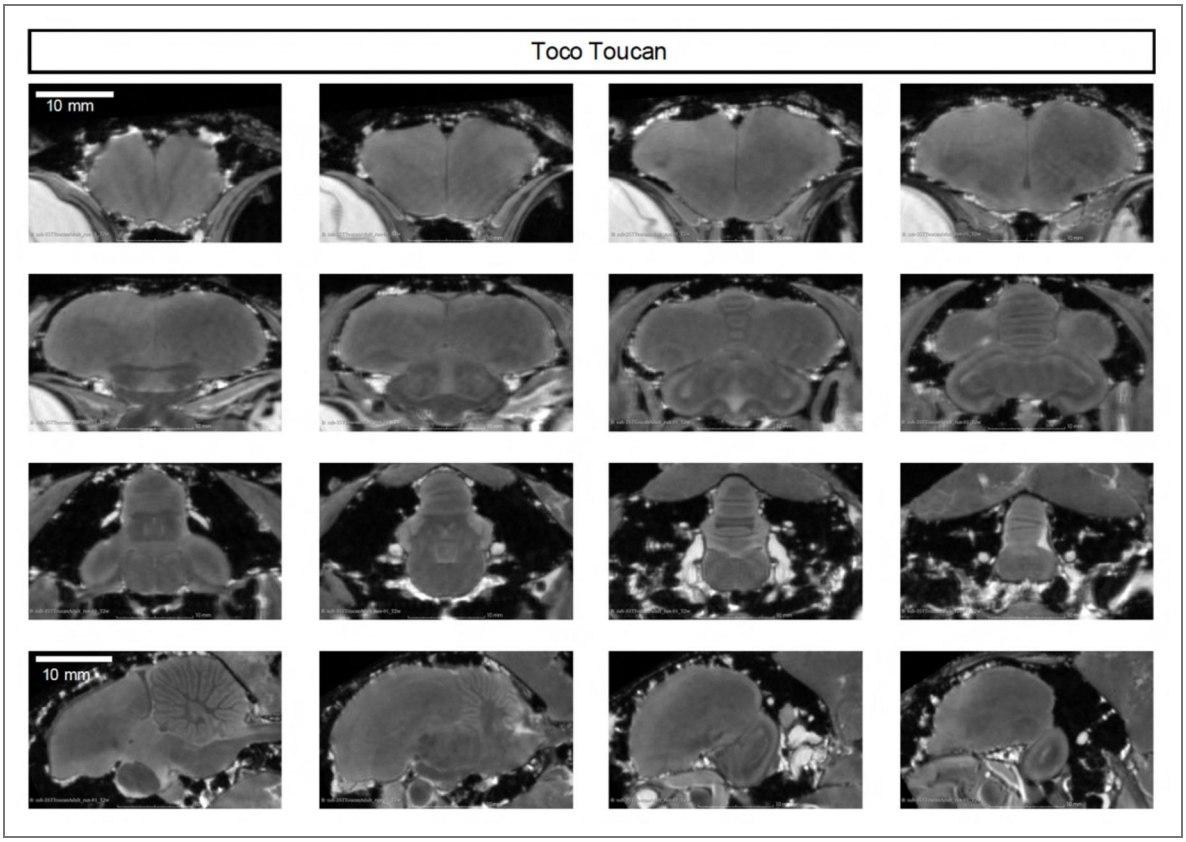

Fig. S12. Serial coronal and sagittal T2-weighted MRI sections of the toco toucan.

Representative serial T2-weighted MRI sections of the toco toucan brain are shown to provide an overview of whole-brain morphology. Consecutive coronal sections are shown together with sagittal sections to illustrate the anatomical continuity of the forebrain, midbrain, cerebellum, and brainstem. Scale bars, 10 mm.

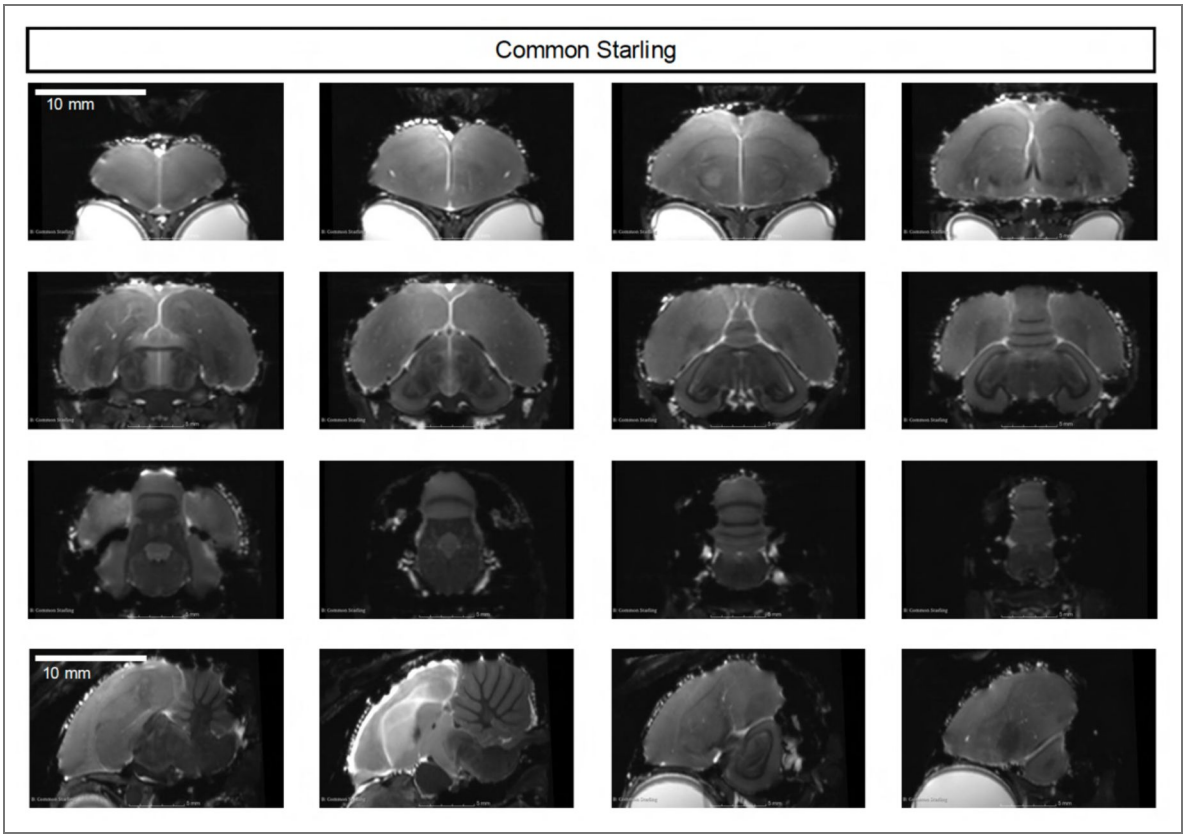

Fig. S13. Serial coronal and sagittal T2-weighted MRI sections of the common starling.

Representative serial T2-weighted MRI sections of the common starling brain are shown to provide an overview of whole-brain morphology. Consecutive coronal sections are shown together with sagittal sections to illustrate the anatomical continuity of the forebrain, midbrain, cerebellum, and brainstem. Scale bars, 10 mm.

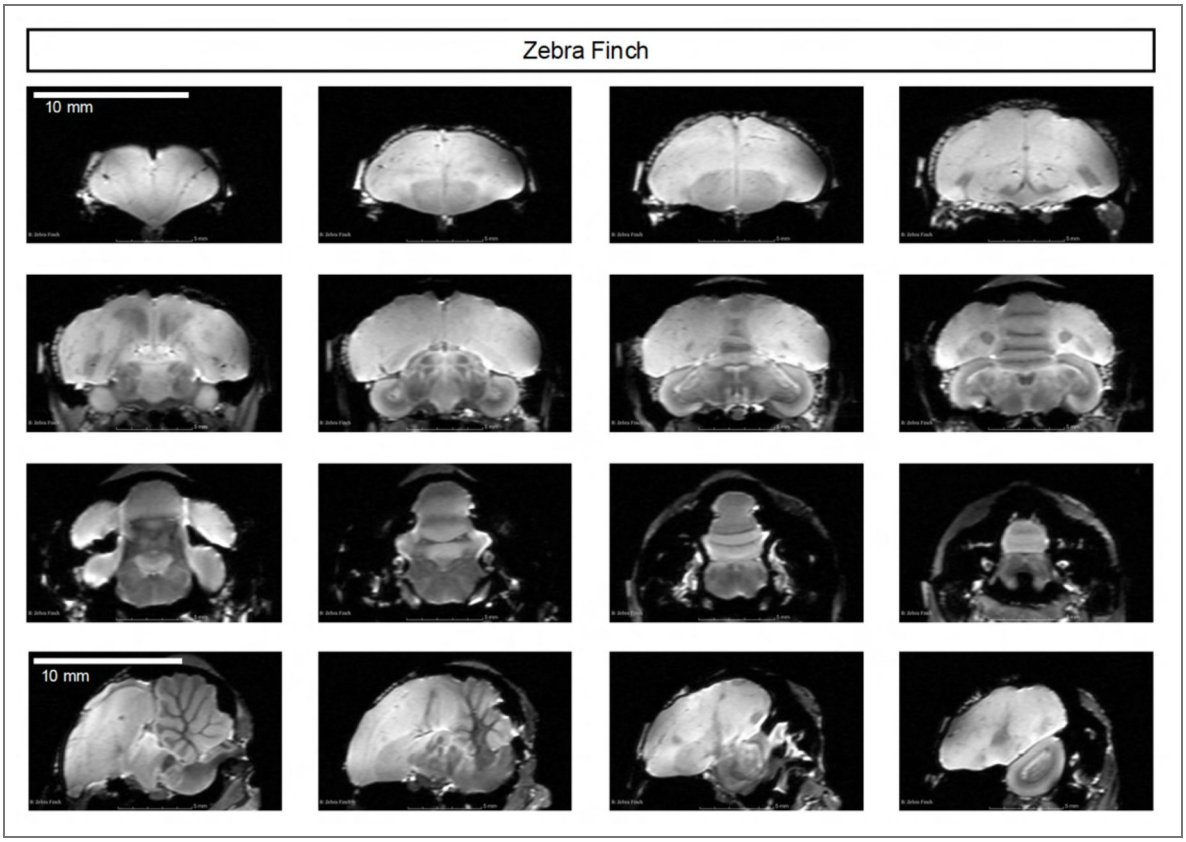

Fig. S14. Serial coronal and sagittal T2-weighted MRI sections of the zebra finch.

Representative serial T2-weighted MRI sections of the zebra finch brain are shown to provide an overview of whole-brain morphology. Consecutive coronal sections are shown together with sagittal sections to illustrate the anatomical continuity of the forebrain, midbrain, cerebellum, and brainstem. Scale bars, 10 mm.

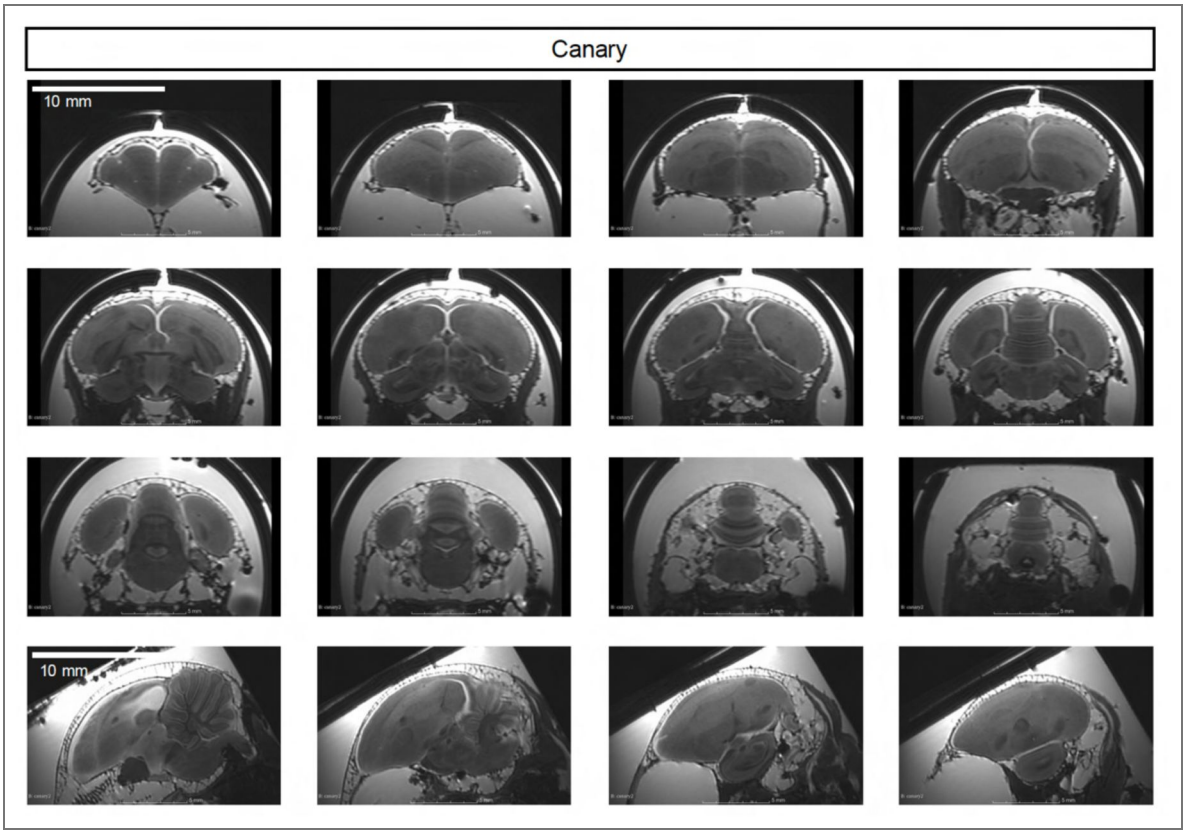

Fig. S15. Serial coronal and sagittal T2-weighted MRI sections of the canary.

Representative serial T2-weighted MRI sections of the canary brain are shown to provide an overview of whole-brain morphology. Consecutive coronal sections are shown together with sagittal sections to illustrate the anatomical continuity of the forebrain, midbrain, cerebellum, and brainstem. Scale bars, 10 mm.

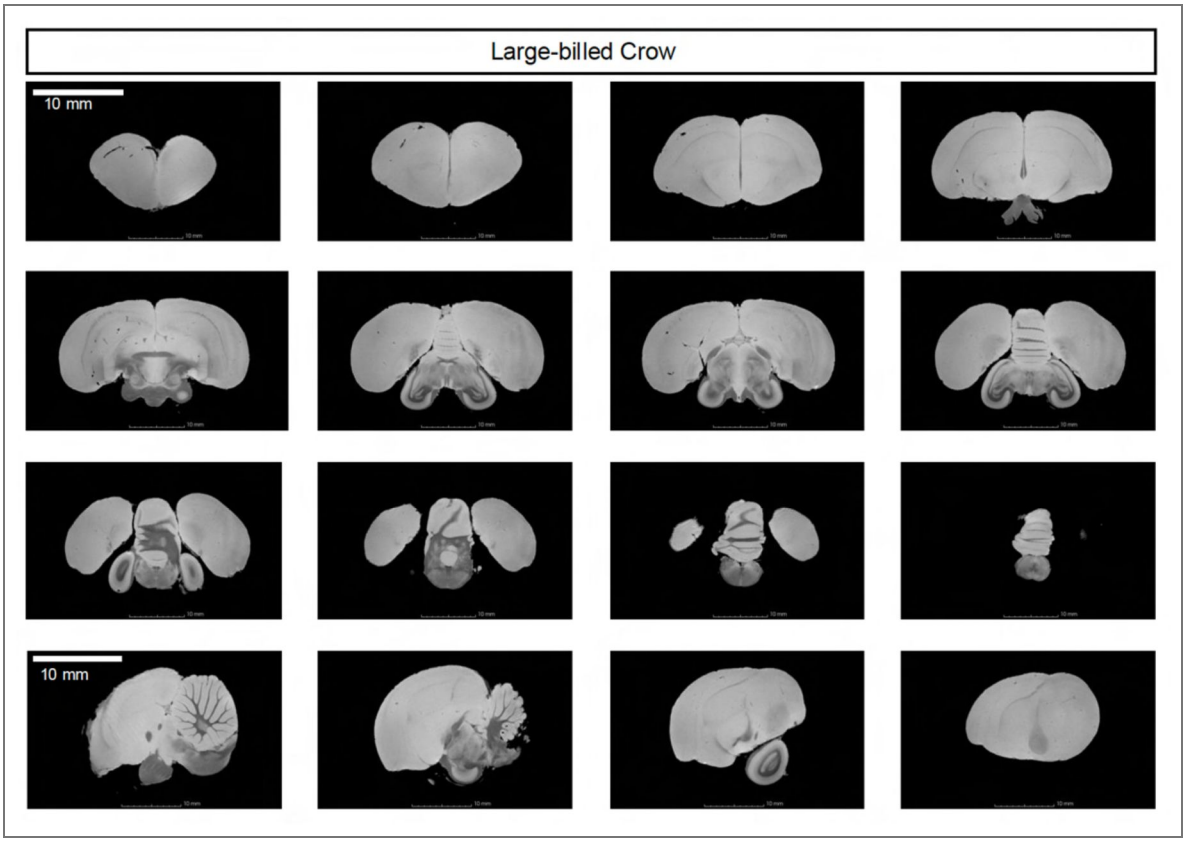

Fig. S16. Serial coronal and sagittal T2-weighted MRI sections of the large-billed crow.

Representative serial T2-weighted MRI sections of the large-billed crow brain are shown to provide an overview of whole-brain morphology. Consecutive coronal sections are shown together with sagittal sections to illustrate the anatomical continuity of the forebrain, midbrain, cerebellum, and brainstem. Scale bars, 10 mm.

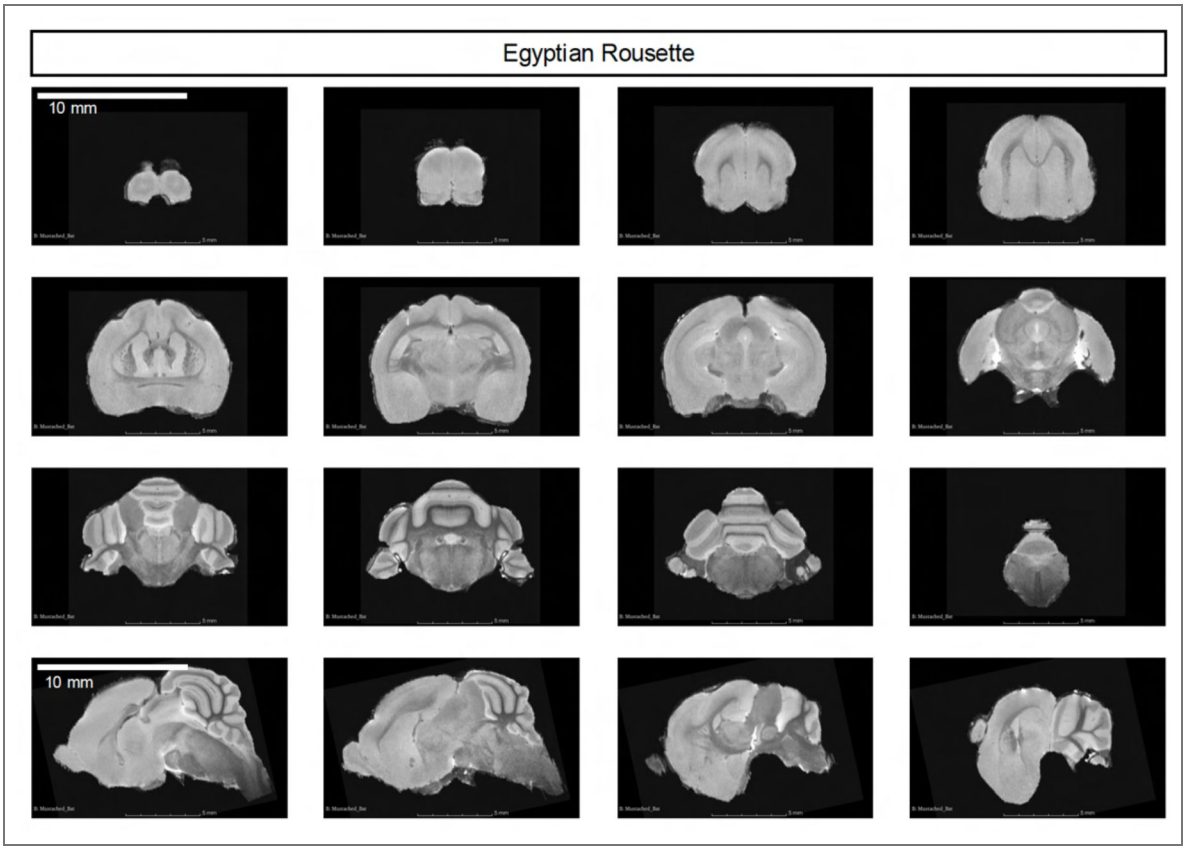

Fig. S17. Serial coronal and sagittal T2-weighted MRI sections of the Egyptian rousette.

Representative serial T2-weighted MRI sections of the Egyptian rousette brain are shown to provide an overview of whole-brain morphology. Consecutive coronal sections are shown together with sagittal sections to illustrate the anatomical continuity of the forebrain, midbrain, cerebellum, and brainstem. Scale bars, 10 mm.

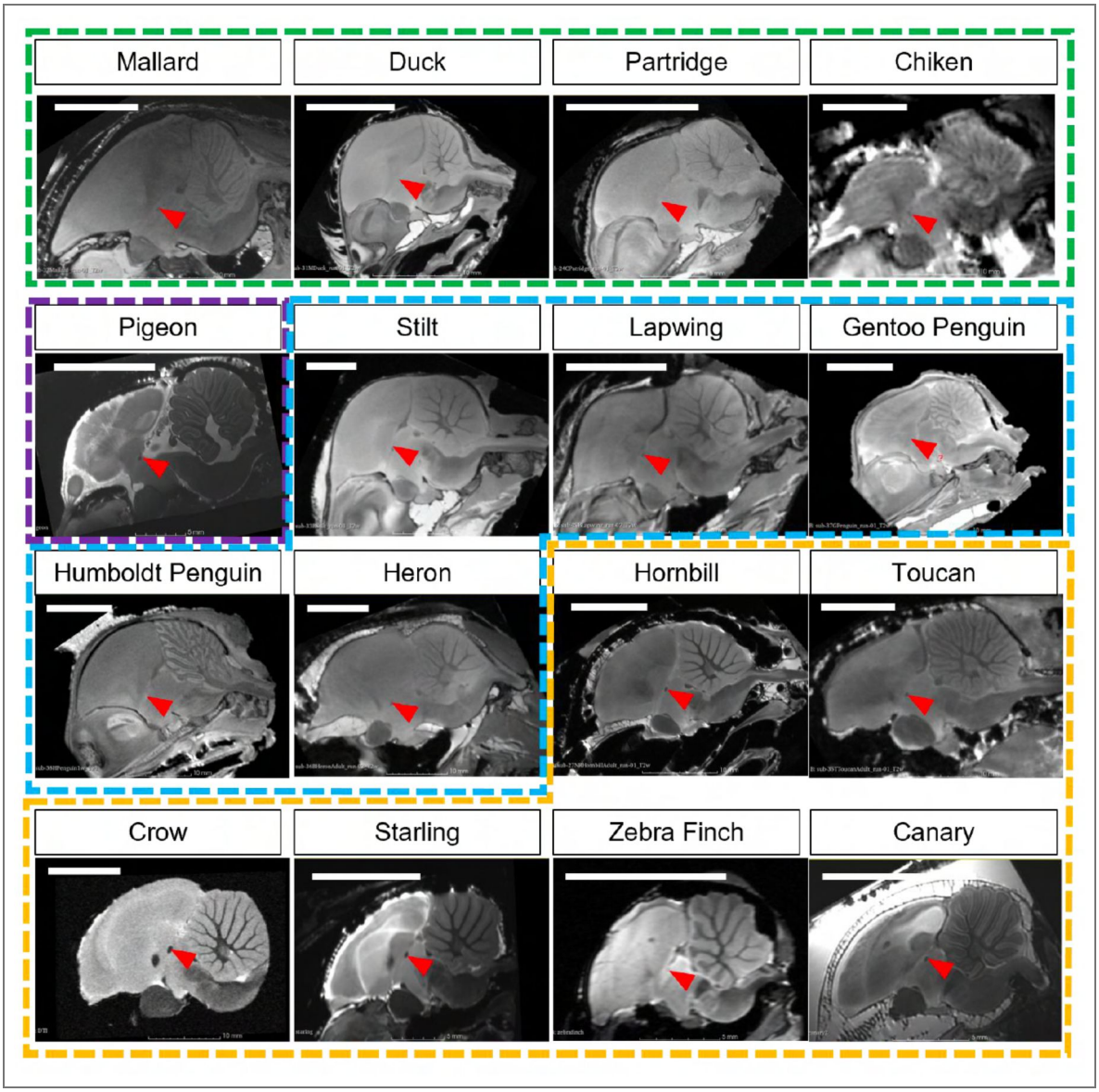

Fig. S18. Sagittal T2-weighted MRI sections showing the anterior commissure across bird species.

Representative sagittal T2-weighted MRI sections used for the analysis shown in Fig. 2A are shown for the examined bird species. The anterior commissure is indicated by red arrowheads. Species are grouped according to the categories used in the main figure. Scale bars, 10 mm.

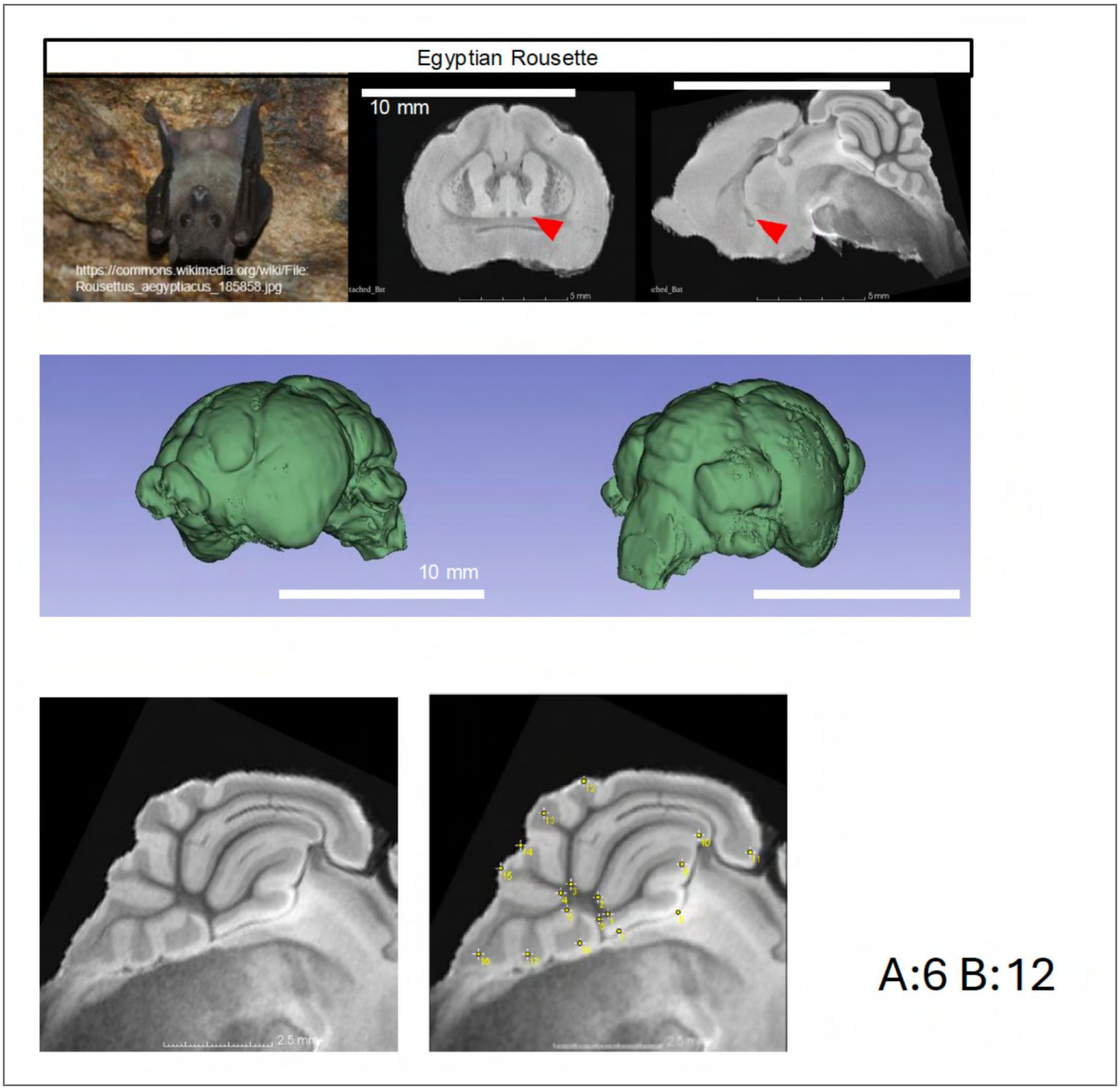

Fig. S19. T2-weighted MRI, three-dimensional reconstruction, and cerebellar foliation analysis of the Egyptian rousette.

Representative T2-weighted MRI sections and three-dimensional surface reconstructions of the Egyptian rousette brain are shown. The anterior commissure is indicated by red arrowheads in the MRI sections. Cerebellar foliation was assessed using sagittal T2-weighted MRI sections, and representative traces used for branch counting are shown. The number of basal branches and terminal branches is indicated as A and B, respectively. Scale bars, 10 mm.

Data availability

The MRI datasets analyzed in this study were obtained from the Animal Brain Collection (ABC) Database and previously published datasets. The ABC MRI datasets are available at *https://togodb.org/db/animal_brain_collection*. The corresponding raw MRI data have been deposited in OpenNeuro and can be accessed through links provided in the ABC Database. Source data files containing the numerical values used to generate the figures are provided as supporting files.

Acknowledgements

The authors would like to thank Drs. Iguchi and Seki, who prepared Nissl and LFB staining samples (TMiMs). This work was supported by a Leading Initiative for Excellent Young Researchers (LEADER) grant (grant number 2020L0019), JSPS KAKENHI grants (20K22665, 22H02638, 23K23901), the FY2021 Research Grant from the Takeda Science Foundation (to T.K.). C.O-M. was supported by JSPS KAKENHI-Grants (25K02289), AMED under Grant Number JP24gm1310012. T.T. was supported by JSPS KAKENHI-Grants (25K02565 and 21K19464). ChatGPT (OpenAI, GPT-5.5 Thinking) was used to assist with English language editing during manuscript preparation.

Additional information

Author contributions

TK designed the research project. YK analyzed MRI images. TT performed MRI analyses. TK wrote the article draft. CO-M supervised the study and revised the manuscript. TK, TT, and CO-M acquired funding. All authors revised the draft manuscript and approved the final version of the manuscript.

Funding

Funder	Grant reference number	Author
MEXT | Japan Society for the Promotion of Science (JSPS)	2020L0019	Takuma Kumamoto
MEXT | Japan Society for the Promotion of Science (JSPS)	20K22665	Takuma Kumamoto
MEXT | Japan Society for the Promotion of Science (JSPS)	22H02638	Takuma Kumamoto
MEXT | Japan Society for the Promotion of Science (JSPS)	23K23901	Takuma Kumamoto
Takeda Science Foundation (TSF)	FY2021	Takuma Kumamoto
MEXT | Japan Society for the Promotion of Science (JSPS)	25K02289	Chiaki Ohtaka-Maruyama
Japan Agency for Medical Research and Development (AMED)	JP24gm1310012	Chiaki Ohtaka-Maruyama
MEXT | Japan Society for the Promotion of Science (JSPS)	25K02565	Tomokazu Tsurugizawa
MEXT | Japan Society for the Promotion of Science (JSPS)	21K19464	Tomokazu Tsurugizawa

Author ORCID iDs

Chiaki Ohtaka-Maruyama: https://orcid.org/0000-0002-0632-7341
Takuma Kumamoto: https://orcid.org/0000-0002-2326-0783

Additional files

Movie 1. Chick.

Movie 2. Crow.

Movie 3. Gentoo Penguin.

Movie 4. Egyptian Rousette.

References

1. **Jarvis ED,** et al. (2005) Avian brains and a new understanding of vertebrate brain evolution. *Nat. Rev. Neurosci* **6**:151-159 https://doi.org/10.1038/nrn1606 | PubMed
2. **Medina L,** Abellán A (2009) Development and evolution of the pallium. *Semin. Cell Dev. Biol* **20**:698-711 https://doi.org/10.1016/j.semcdb.2009.04.008 | PubMed
3. **Olkowicz S,** et al. (2016) Birds have primate-like numbers of neurons in the forebrain. *Proc. Natl. Acad. Sci. U. S. A* **113**:7255-7260 https://doi.org/10.1073/pnas.1517131113 | PubMed
4. **Konishi M,** Emlen ST, Ricklefs RE, Wingfield JC (1989) Contributions of bird studies to biology. *Science* **246**:465-472 https://doi.org/10.1126/science.2683069 | PubMed
5. **Wylie DR,** Gutiérrez-Ibáñez C, Iwaniuk AN (2015) Integrating brain, behavior, and phylogeny to understand the evolution of sensory systems in birds. *Front. Neurosci* **9**:281 https://doi.org/10.3389/fnins.2015.00281 | PubMed
6. **Vincze O,** Vágási CI, Pap PL, Osváth G, Møller AP (2015) Brain regions associated with visual cues are important for bird migration. *Biol. Lett* **11**:20150678 https://doi.org/10.1098/rsbl.2015.0678 | PubMed
7. **Corfield JR,** et al. (2015) Diversity in olfactory bulb size in birds reflects allometry, ecology, and phylogeny. *Front. Neuroanat* **9**:102 https://doi.org/10.3389/fnana.2015.00102 | PubMed
8. **Jarvis ED** (2004) Learned birdsong and the neurobiology of human language. *Ann. N. Y. Acad. Sci* **1016**:749-777 https://doi.org/10.1196/annals.1298.038 | PubMed
9. **De Groof G,** Van der Linden A (2010) Love songs, bird brains and diffusion tensor imaging: DTI OF BRAIN PLASTICITY IN SONGBIRDS. *NMR Biomed* **23**:873-883 https://doi.org/10.1002/nbm.1551 | PubMed
10. **Balanoff AM,** et al. (2016) Best practices for digitally constructing endocranial casts: examples from birds and their dinosaurian relatives. *J. Anat* **229**:173-190 https://doi.org/10.1111/joa.12378 | PubMed
11. **Poirier C,** et al. (2008) A three-dimensional MRI atlas of the zebra finch brain in stereotaxic coordinates. *Neuroimage* **41**:1-6 https://doi.org/10.1016/j.neuroimage.2008.01.069 | PubMed
12. **De Groof G,** et al. (2006) In vivo diffusion tensor imaging (DTI) of brain subdivisions and vocal pathways in songbirds. *Neuroimage* **29**:754-763 https://doi.org/10.1016/j.neuroimage.2005.09.022 | PubMed
13. **Tsurugizawa T,** et al. (2025) A cross-species brain magnetic resonance imaging and histology database of vertebrates. *Sci. Data* **12**:1206 https://doi.org/10.1038/s41597-025-05540-5 | PubMed
14. **Van der Linden A,** et al. (1998) Non invasive in vivo anatomical studies of the oscine brain by high resolution MRI microscopy. *J. Neurosci. Methods* **81**:45-52 https://doi.org/10.1016/s0165-0270(98)00013-2 | PubMed
15. **Güntürkün O,** Verhoye M, De Groof G, Van der Linden A (2013) A 3-dimensional digital atlas of the ascending sensory and the descending motor systems in the pigeon brain. *Brain Struct. Funct* **218**:269-281 https://doi.org/10.1007/s00429-012-0400-y | PubMed
16. **De Groof G,** et al. (2016) A three-dimensional digital atlas of the starling brain. *Brain Struct. Funct* **221**:1899-1909 https://doi.org/10.1007/s00429-015-1011-1 | PubMed

17. **Letzner S,** Simon A, Güntürkün O (2016) Connectivity and neurochemistry of the commissura anterior of the pigeon (Columba livia): Connectivity and neurochemistry of pigeon AC. *J. Comp. Neurol* **524**:343-361 https://doi.org/10.1002/cne.23858 | PubMed

18. **Ksepka DT,** et al. (2020) Tempo and Pattern of Avian Brain Size Evolution. *Curr. Biol* **30**:2026-2036.e3 https://doi.org/10.1016/j.cub.2020.03.060 | PubMed

19. **Early CM,** Iwaniuk AN, Ridgely RC, Witmer LM (2020) Endocast structures are reliable proxies for the sizes of corresponding regions of the brain in extant birds. *J. Anat* **237**:1162-1176 https://doi.org/10.1111/joa.13285 | PubMed

20. **Kverková K,** et al. (2022) The evolution of brain neuron numbers in amniotes. *Proc. Natl. Acad. Sci. U. S. A* **119**:e2121624119 https://doi.org/10.1073/pnas.2121624119 | PubMed

21. **Yebga Hot R,** et al. (2022) A novel male Japanese quail structural connectivity atlas using ultra-high field diffusion MRI at 11.7 T. *Brain Struct. Funct* **227**:1577-1597 https://doi.org/10.1007/s00429-022-02457-2 | PubMed

22. **Jeurissen B,** Descoteaux M, Mori S, Leemans A (2019) Diffusion MRI fiber tractography of the brain. *NMR Biomed* **32**:e3785 https://doi.org/10.1002/nbm.3785 | PubMed

23. **Hardie JL,** Cooney CR (2023) Sociality, ecology and developmental constraints predict variation in brain size across birds. *J. Evol. Biol* **36**:144-155 https://doi.org/10.1111/jeb.14117 | PubMed

24. **Fristoe TS,** Botero CA (2019) Alternative ecological strategies lead to avian brain size bimodality in variable habitats. *Nat. Commun* **10**:3818 https://doi.org/10.1038/s41467-019-11757-x | PubMed

25. **Shiomi K** (2022) Possible link between brain size and flight mode in birds: Does soaring ease the energetic limitation of the brain?. *Evolution* **76**:649-657 https://doi.org/10.1111/evo.14425 | PubMed

26. **Vincze O** (2016) Light enough to travel or wise enough to stay? Brain size evolution and migratory behavior in birds: BRAIN SIZE EVOLUTION AND MIGRATION IN BIRDS. *Evolution* **70**:2123-2133 https://doi.org/10.1111/evo.13012 | PubMed

27. **Sayol F,** et al. (2016) Environmental variation and the evolution of large brains in birds. *Nat. Commun* **7**:13971 https://doi.org/10.1038/ncomms13971 | PubMed

28. **Garamszegi LZ,** Møller AP, Erritzøe J (2002) Coevolving avian eye size and brain size in relation to prey capture and nocturnality. *Proc. Biol. Sci* **269**:961-967 https://doi.org/10.1098/rspb.2002.1967 | PubMed

29. **Samia DSM,** Pape Møller A, Blumstein DT (2015) Brain size as a driver of avian escape strategy. *Sci. Rep* **5**:11913 https://doi.org/10.1038/srep11913 | PubMed

30. **Burish MJ,** Kueh HY, Wang SS.-H (2004) Brain architecture and social complexity in modern and ancient birds. *Brain Behav. Evol* **63**:107-124 https://doi.org/10.1159/000075674 | PubMed

31. **Houle L,** Larouche O, Cloutier R (2026) Exploring larval axolotl brain development: Insights into developmental and functional constraints. *Evol. Dev* **28**:e70034 https://doi.org/10.1111/ede.70034 | PubMed

32. **Kawabe S,** Matsuda S, Tsunekawa N, Endo H (2015) Ontogenetic shape change in the chicken brain: Implications for paleontology. *PLoS One* **10**:e0129939 https://doi.org/10.1371/journal.pone.0129939 | PubMed

33. **Zhou Z,** et al. (2020) Evaluation of the diffusion MRI white matter tract integrity model using myelin histology and Monte-Carlo simulations. *Neuroimage* **223**:117313 https://doi.org/10.1016/j.neuroimage.2020.117313 | PubMed

34. **Mukherjee P,** McKinstry RC (2006) Diffusion tensor imaging and tractography of human brain development. *Neuroimaging Clin. N. Am* **16**:19-43 https://doi.org/10.1016/j.nic.2005.11.004 | PubMed

35. **Nomura T,** Gotoh H, Ono K (2013) Changes in the regulation of cortical neurogenesis contribute to encephalization during amniote brain evolution. *Nat. Commun* **4**:2206 https://doi.org/10.1038/ncomms3206 | PubMed

36. **Cárdenas A,** Borrell V (2020) Molecular and cellular evolution of corticogenesis in amniotes. *Cell. Mol. Life Sci* **77**:1435-1460 https://doi.org/10.1007/s00018-019-03315-x | PubMed

Tsurugizawa T, et al (2025) A cross-species brain magnetic resonance imaging and histology database of vertebrates. ToGoDB and OpenNeuro. https://togodb.org/db/animal_brain_collection

Güntürkün O, Verhoye M, De Groof G, Van der Linden A (2013) A 3-dimensional digital atlas of the ascending sensory and the descending motor systems in the pigeon brain. Published MRI/CT atlas dataset; pigeon. https://www.bio.psy.ruhr-uni-bochum.de/bpsy/research/opensoftware/3dml_pigeon_manual.html.en

Peer reviews

Reviewer #1 (Public review):

Summary:

The study presents a novel analysis of MRI resources for 16 avian species, spanning major (though not all) clades and ecological niches. This is a significant step towards large-scale datasets on internal parcellation and long-range connectivity, central to evolutionary studies for understanding the evolution of the bird brain.

Strengths:

The integration of high-resolution T2-weighted and diffusion-weighted MRI with histological validation (Nissl and Luxol Fast Blue staining) provides a strong, cross-validated framework for studying avian brain anatomy. Data on long-range connectivity are particularly useful for understanding how relationships between brain components evolved. The approach is also scalable, allowing for more detailed evolutionary analyses compared to what is currently possible.

Weaknesses:

The sampling supports evidence of modular evolution in the bird brain, but it is limited for broad evolutionary claims, as the effects of sizes and phylogenies can be hard to disentangle without enough species per clade.

Tractography-based claims should be treated cautiously without sensitivity analyses. This is particularly important when comparing brains with different sizes and tissue properties.

Existing literature is not acknowledged sufficiently. This makes some claims of novelty misleading, and prevents readers from understanding the current state of knowledge in this research area.

https://doi.org/10.7554/eLife.112415.1.sa2

Reviewer #2 (Public review):

This manuscript presents a comparative MRI dataset from 16 avian species and uses MRI and tractography to examine variation in brain organization across birds. The authors argue that their analyses support mosaic brain evolution and provide a framework for comparative neuroanatomy. Although the dataset represents a useful resource, particularly given the inclusion of understudied species like penguins, toucans, and hornbills, I have substantial concerns regarding the novelty of the study, the anatomical interpretation of the results, and the validity of the tractography analyses. In its current form, I do not believe the manuscript provides sufficient new biological insight to support many of its conclusions.

Major Concerns

(1) The authors repeatedly state that comparative neuroanatomical studies in birds have largely been unable to examine internal brain organization or "internal parcellation". This claim is inaccurate and reflects limited engagement with a substantial body of literature. For decades, comparative studies have examined variation in the size of major avian brain subdivisions as well as specific sensory, motor, and associative nuclei. For example, the extensive work of Andrew Iwaniuk and colleagues has documented variation in numerous brain regions across birds and related these differences to ecology, behavior, and sensory specialization (e.g., Gutierrez-Ibanez et al., 2009; Iwaniuk et al., 2006, 2008, 2010; Corfield et al., 2015). Other authors have also made important contributions in this area (e.g., Boire and Baron, 1994; Burish et al., 2004; Moore and DeVoogd, 2011, 2017). Importantly, previous work has already examined variation in major subdivisions of the avian brain using relatively standardized datasets (e.g., Iwaniuk et al., 2004; Iwaniuk and Hurd, 2005), including datasets that contain more species and greater taxonomic diversity than the current study. In other words, these studies have already provided detailed analyses of internal brain organization across broad taxonomic samples.

The manuscript should therefore be reframed as providing a new MRI-based resource rather than introducing the first comparative framework for studying internal avian brain organization. The current framing significantly overstates the novelty of the work.

(2) A second significant concern is the lack of anatomical specificity in the tractography analyses. The authors repeatedly refer to regions such as "anterior cortex," "dorsal cortex," and "temporal cortex." These terms are not standard anatomical designations in avian neuroanatomy and provide little information about the actual structures being analyzed.

For example, the "temporal cortex" could potentially include portions of the nidopallium (including the caudolateral nidopallium, NCL), mesopallium, and arcopallium. Similarly, the "anterior cortex" could correspond to the somatosensory or visual Wulst, the anterior nidopallium, or several other structures. The designation "dorsal cortex" is similarly difficult to interpret. Because these seed regions may encompass multiple functionally distinct systems, it is impossible to evaluate the biological significance of the reported connectivity patterns.

I strongly encourage the authors to define their seed regions using accepted avian neuroanatomical terminology and to provide detailed anatomical maps. More informative analyses would focus on well-defined structures with known connectivity, such as the Wulst, arcopallium, entopallium, or NCL. As currently presented, the tractography results are too coarse to support meaningful biological conclusions.

(3) I am not an MRI specialist, but I have concerns regarding the interpretation of the tractography results. Bird brains are small, and diffusion MRI tractography is already known to be challenging even in substantially larger brains. The manuscript provides limited information regarding image resolution, diffusion sampling, and the expected accuracy of tract reconstruction in these specimens. More importantly, there is little validation of the tractography results. Diffusion tractography is prone to both false positives and false negatives, and reconstructed pathways cannot be assumed to represent true anatomical connections.

The authors should provide evidence that their tractography pipeline can accurately recover known pathways. For example, they could compare reconstructed tracts with well-established anatomical pathways such as the anterior commissure or major visual pathways, which would substantially strengthen confidence in the results. Without such validation, it is difficult to determine whether the observed species differences reflect biological variation or methodological artifacts.

(4) I also have some methodological concerns regarding the comparisons of anterior commissure (AC) size and cerebellar foliation. First, the authors measure the AC in a coronal section. I would recommend measuring the AC area in a midsagittal section instead. Furthermore, the authors use the cross-sectional area of the same coronal section as the scaling variable. This seems problematic because the area of any given section will depend on the angle of sectioning and other technical factors. If the objective is to compare the relative size of the AC, then total brain volume or telencephalon volume would be more appropriate scaling variables.

With respect to cerebellar foliation, the authors developed their own metric. I would encourage them to use methods already established in the literature, such as the foliation index described by Iwaniuk et al. (2006). Their approach may yield similar results, but using the foliation index would facilitate direct comparisons with existing datasets and would allow incorporation of additional published data (e.g., Cunha et al., 2021, which includes foliation index measurements for 54 bird species). The authors should also be aware that the foliation index scales with body size. Consequently, the high degree of foliation observed in penguins may not necessarily indicate cerebellar expansion or increased demands for sensorimotor integration associated with their specialized locomotion. I therefore believe that the conclusions regarding variation in AC size and cerebellar foliation should be re-evaluated after more appropriate analyses are performed.

https://doi.org/10.7554/eLife.112415.1.sa1

Author response:

> ***Public Reviews:***
>
> ***Reviewer #1 (Public review):***
>
> *Summary:*
>
> *The study presents a novel analysis of MRI resources for 16 avian species, spanning major (though not all) clades and ecological niches. This is a significant step towards large-scale datasets on internal parcellation and long-range connectivity, central to evolutionary studies for understanding the evolution of the bird brain.*
>
> *Strengths:*
>
> *The integration of high-resolution T2-weighted and diffusion-weighted MRI with histological validation (Nissl and Luxol Fast Blue staining) provides a strong, cross-validated framework for studying avian brain anatomy. Data on long-range connectivity are particularly useful for understanding how relationships between brain components evolved. The approach is also scalable, allowing for more detailed evolutionary analyses compared to what is currently possible.*
>
> *Weaknesses:*
>
> *The sampling supports evidence of modular evolution in the bird brain, but it is limited for broad evolutionary claims, as the effects of sizes and phylogenies can be hard to disentangle without enough species per clade.*

We appreciate the reviewer highlighting this limitation and agree that it warrants explicit consideration. Although the 16 species included in the current study encompass diverse avian lineages and ecological characteristics, our sampling was not designed to rigorously disentangle the effects of phylogeny and brain size within individual clades.

To improve the taxonomic coverage of our dataset, we plan to expand the MRI dataset in the revised manuscript by including additional specimens that are currently available to us. Specifically, we will acquire and analyze MRI data from the slaty-backed gull (Larus schistisagus), black-tailed gull (Larus crassirostris), budgerigar (Melopsittacus undulatus), and crow (Corvus sp.). In addition, we plan to incorporate publicly available MRI data from the ostrich (Struthio camelus). These additions will broaden the phylogenetic and anatomical coverage of the comparative dataset.

Nevertheless, we fully acknowledge the reviewer's point that, even with these additional species, the number of species sampled within individual clades will remain insufficient to rigorously separate phylogenetic effects from size-related effects or to support broad generalizations across all avian lineages. We will therefore explicitly state this limitation in the revised manuscript and temper evolutionary claims that extend beyond what can be supported by the present taxonomic sampling.

Accordingly, we will more clearly position the primary contribution of this study as the establishment of an MRI-based comparative resource and analytical framework applicable across diverse avian species, rather than as a comprehensive phylogenetic test of avian brain evolution. Within this scope, we will present the observed variation among brain compartments as evidence consistent with mosaic/modular diversification, while carefully limiting the broader evolutionary interpretation of these patterns.

> *Tractography-based claims should be treated cautiously without sensitivity analyses. This is particularly important when comparing brains with different sizes and tissue properties.*

The reviewer raises an important point regarding the interpretation of tractography-based comparisons. We agree that particular caution is required when comparing datasets across species that differ in brain size, tissue properties, and imaging characteristics.

In the revised manuscript, we will perform additional sensitivity analyses to evaluate the robustness of the major tractography-derived patterns. Specifically, we will examine the effects of varying the FA threshold used for tract reconstruction, rather than relying solely on the current threshold of 0.1, and assess whether the major reconstructed trajectory patterns and cross-species differences are robust to this parameter.

We will also re-analyze the available diffusion data using Generalized Q-Sampling Imaging (GQI) as an alternative reconstruction approach and compare the resulting trajectory patterns with those obtained using the current DTI-based analysis. We recognize that the ability to resolve complex fiber configurations depends on the underlying diffusion acquisition parameters, including b-value and spatial and angular resolution. We will therefore interpret these comparisons within the limitations of the currently available datasets, without implying that either reconstruction approach provides a definitive representation of the underlying fiber architecture.

In addition, we will provide a more detailed description of the relevant diffusion MRI acquisition parameters and spatial and angular resolution of the datasets so that potential technical differences among species can be more clearly evaluated. We will also discuss how such differences may affect cross-species tractography comparisons.

Finally, we will revise the interpretation of the tractography results throughout the manuscript to more clearly distinguish diffusion MRI-derived reconstructed trajectories from anatomically demonstrated neuronal connections. We will avoid treating reconstructed streamlines as direct evidence of anatomical connectivity and will explicitly discuss the potential for false-positive and false-negative tract reconstruction, as well as other limitations inherent to diffusion MRI tractography.

> *Existing literature is not acknowledged sufficiently. This makes some claims of novelty misleading, and prevents readers from understanding the current state of knowledge in this research area.*

We fully agree with this assessment. Although substantial comparative neuroanatomical work has established important principles of avian brain evolution, the current manuscript does not sufficiently cite or incorporate this literature into the discussion. As a result, some statements regarding the novelty of the present study are overstated.

In the revised manuscript, we will substantially expand our discussion and citation of the relevant literature, including the extensive comparative studies of individual avian brain regions and brain subdivisions highlighted by the reviewers. We will revise the Introduction and Discussion accordingly to more accurately describe the current state of knowledge in comparative avian neuroanatomy and to clearly distinguish the contributions of previous studies from those of the present work.

We will also carefully revise statements regarding the novelty of our study. Rather than implying that our study provides the first comparative framework for examining internal avian brain organization, we will more appropriately emphasize its contribution as an MRI-based comparative resource that enables standardized visualization and analysis of internal brain anatomy and connectivity across diverse avian species.

Reviewer #2 (Public review):

This manuscript presents a comparative MRI dataset from 16 avian species and uses MRI and tractography to examine variation in brain organization across birds. The authors argue that their analyses support mosaic brain evolution and provide a framework for comparative neuroanatomy. Although the dataset represents a useful resource, particularly given the inclusion of understudied species like penguins, toucans, and hornbills, I have substantial concerns regarding the novelty of the study, the anatomical interpretation of the results, and the validity of the tractography analyses. In its current form, I do not believe the manuscript provides sufficient new biological insight to support many of its conclusions.

Major Concerns

(1) The authors repeatedly state that comparative neuroanatomical studies in birds have largely been unable to examine internal brain organization or "internal parcellation". This claim is inaccurate and reflects limited engagement with a substantial body of literature. For decades, comparative studies have examined variation in the size of major avian brain subdivisions as well as specific sensory, motor, and associative nuclei. For example, the extensive work of Andrew Iwaniuk and colleagues has documented variation in numerous brain regions across birds and related these differences to ecology, behavior, and sensory specialization (e.g., Gutierrez-Ibanez et al., 2009; Iwaniuk et al., 2006, 2008, 2010; Corfield et al., 2015). Other authors have also made important contributions in this area (e.g., Boire and Baron, 1994; Burish et al., 2004; Moore and DeVoogd, 2011, 2017). Importantly, previous work has already examined variation in major subdivisions of the avian brain using relatively standardized datasets (e.g., Iwaniuk et al., 2004; Iwaniuk and Hurd, 2005), including datasets that contain more species and greater taxonomic diversity than the current study. In other words, these studies have already provided detailed analyses of internal brain organization across broad taxonomic samples.

The manuscript should therefore be reframed as providing a new MRI-based resource rather than introducing the first comparative framework for studying internal avian brain organization. The current framing significantly overstates the novelty of the work.

We appreciate the reviewer drawing attention to this issue. Although a substantial body of comparative neuroanatomical work has already examined internal brain organization in birds, the current manuscript does not sufficiently cite or incorporate this literature into the discussion. As a consequence, some statements regarding the novelty of our study are overstated.

In the revised manuscript, we will expand our discussion and citation of previous work, including the studies highlighted by the reviewer on interspecific variation in major avian brain subdivisions, sensory and motor nuclei, and other anatomically defined brain regions. We will revise the Introduction and Discussion to more accurately represent the existing body of comparative avian neuroanatomy and to clarify how the present study complements and extends these established approaches.

Most importantly, we will reframe the manuscript so that its primary contribution is presented as the establishment of an MRI-based comparative resource for visualizing and quantitatively analyzing internal brain anatomy across diverse avian species. We will remove or revise statements implying that the present study provides the first comparative framework for examining internal avian brain organization. Instead, we will emphasize the complementary advantages of the MRI-based approach, particularly its ability to provide non-destructive three-dimensional visualization of internal brain structures in intact

specimens and to enable comparison of multiple brain compartments within a common analytical framework across diverse avian species.

We believe that this revised framing will more accurately position the contribution of our study within the existing literature and clarify the specific value of the dataset.

> *(2) A second significant concern is the lack of anatomical specificity in the tractography analyses. The authors repeatedly refer to regions such as "anterior cortex," "dorsal cortex," and "temporal cortex." These terms are not standard anatomical designations in avian neuroanatomy and provide little information about the actual structures being analyzed.*
>
> *For example, the "temporal cortex" could potentially include portions of the nidopallium (including the caudolateral nidopallium, NCL), mesopallium, and arcopallium. Similarly, the "anterior cortex" could correspond to the somatosensory or visual Wulst, the anterior nidopallium, or several other structures. The designation "dorsal cortex" is similarly difficult to interpret. Because these seed regions may encompass multiple functionally distinct systems, it is impossible to evaluate the biological significance of the reported connectivity patterns.*
>
> *I strongly encourage the authors to define their seed regions using accepted avian neuroanatomical terminology and to provide detailed anatomical maps. More informative analyses would focus on well-defined structures with known connectivity, such as the Wulst, arcopallium, entopallium, or NCL. As currently presented, the tractography results are too coarse to support meaningful biological conclusions.*

This is an important concern, and we agree that the anatomical nomenclature and definition of the regions used in the tractography analyses require substantial improvement.

In the revised manuscript, we will carefully re-evaluate the anatomical description of each region with reference to established avian neuroanatomical terminology, anatomical atlases, and available histological information. Where the analyzed regions can be reliably assigned to established anatomical structures, we will replace broad mammalian-style positional terminology such as “anterior cortex,” “dorsal cortex,” and “temporal cortex” with more appropriate avian neuroanatomical terminology. For example, we will re-examine whether the region currently referred to as the “optic lobe” can be more precisely defined as the optic tectum, while the cerebellum can be retained as an anatomically well-defined region.

At the same time, we recognize an important limitation of the present tractography analysis. The spatial resolution and analytical framework of the present comparative datasets do not necessarily permit reliable assignment of all analyzed regions or reconstructed trajectory patterns to fine pallial subdivisions such as the entopallium, arcopallium, or NCL across species. We therefore do not intend to assign such specific anatomical identities where they cannot be supported with sufficient confidence.

Instead, for regions that cannot be unambiguously assigned to a single established anatomical subdivision, we will define their location and extent using reproducible anatomical landmarks and clearly indicate the level of anatomical resolution supported by the data. We will also provide revised anatomical maps showing the locations of the analyzed regions and their relationship to major avian brain subdivisions. This will allow readers to evaluate more clearly which anatomical structures may contribute to the reconstructed trajectory patterns.

Accordingly, we will revise the biological interpretation of the tractography results to match this anatomical resolution. Rather than attributing the reconstructed patterns to specific fine-scale pallial structures or functional systems when these cannot be reliably distinguished, we will interpret them more conservatively as broad patterns of fibre organisation among

anatomically defined brain regions. These revisions will improve the anatomical transparency of the analysis while avoiding anatomical or functional interpretations that exceed the resolution of the present datasets.

> *(3) I am not an MRI specialist, but I have concerns regarding the interpretation of the tractography results. Bird brains are small, and diffusion MRI tractography is already known to be challenging even in substantially larger brains. The manuscript provides limited information regarding image resolution, diffusion sampling, and the expected accuracy of tract reconstruction in these specimens. More importantly, there is little validation of the tractography results. Diffusion tractography is prone to both false positives and false negatives, and reconstructed pathways cannot be assumed to represent true anatomical connections.*
>
> *The authors should provide evidence that their tractography pipeline can accurately recover known pathways. For example, they could compare reconstructed tracts with well-established anatomical pathways such as the anterior commissure or major visual pathways, which would substantially strengthen confidence in the results. Without such validation, it is difficult to determine whether the observed species differences reflect biological variation or methodological artifacts.*

We agree with the reviewer that the tractography results require cautious interpretation and that further evaluation of the robustness and anatomical plausibility of the tractography pipeline would strengthen the study.

In the revised manuscript, we will provide a more detailed description of the diffusion MRI acquisition parameters, spatial and angular resolution, diffusion reconstruction, and tractography procedures so that the methodological limitations of the analyses can be more clearly assessed.

Recent studies using DTI under imaging conditions comparable to those employed in the present study have demonstrated successful reconstruction of fiber trajectories in the mouse brain, which is smaller than the avian brains examined here (Janz et al., eLife, 2017). We therefore consider that the size of the avian brain itself does not preclude DTI-based fiber reconstruction and that such analyses are technically feasible at the brain sizes examined in the present study.

Importantly, we will perform additional sensitivity analyses to evaluate the robustness of the reconstructed trajectory patterns. Specifically, we will examine the effects of varying the FA threshold used for tract reconstruction. We will also re-analyse the available diffusion data using Generalized Q-Sampling Imaging (GQI) as an alternative reconstruction approach and compare the resulting trajectory patterns with those obtained using the current DTI-based analysis. We recognize that the ability to resolve complex fiber configurations depends on the diffusion acquisition parameters, including b-value and spatial and angular resolution. We will therefore interpret the comparison between reconstruction approaches within the limitations of the currently available datasets, without implying that either approach provides a definitive reconstruction of the underlying fiber architecture.

We will also evaluate the robustness of the k-means clustering used to summarize tractography patterns. Because the current choice of k = 10 was not based on an independently established biological criterion, we will examine alternative values of k and assess whether the major trajectory patterns and cross-species differences are robust to the choice of cluster number.

In addition, we will examine anatomically well-characterized pathways, including major commissural and visual pathways, and assess whether the reconstructed trajectories are consistent with known avian neuroanatomy. We will use these comparisons as an assessment of anatomical plausibility rather than as definitive validation of tractography accuracy.

Finally, we will revise the manuscript to more clearly distinguish diffusion MRI-derived reconstructed trajectories from anatomically demonstrated neuronal connections. We will avoid interpreting reconstructed streamlines as direct evidence of anatomical connectivity and will explicitly discuss the possibility of false-positive and false-negative tract reconstruction, as well as other limitations inherent to diffusion MRI tractography.

> *(4) I also have some methodological concerns regarding the comparisons of anterior commissure (AC) size and cerebellar foliation. First, the authors measure the AC in a coronal section. I would recommend measuring the AC area in a midsagittal section instead. Furthermore, the authors use the cross-sectional area of the same coronal section as the scaling variable. This seems problematic because the area of any given section will depend on the angle of sectioning and other technical factors. If the objective is to compare the relative size of the AC, then total brain volume or telencephalon volume would be more appropriate scaling variables.*
>
> *With respect to cerebellar foliation, the authors developed their own metric. I would encourage them to use methods already established in the literature, such as the foliation index described by Iwaniuk et al. (2006). Their approach may yield similar results, but using the foliation index would facilitate direct comparisons with existing datasets and would allow incorporation of additional published data (e.g., Cunha et al., 2021, which includes foliation index measurements for 54 bird species). The authors should also be aware that the foliation index scales with body size. Consequently, the high degree of foliation observed in penguins may not necessarily indicate cerebellar expansion or increased demands for sensorimotor integration associated with their specialized locomotion. I therefore believe that the conclusions regarding variation in AC size and cerebellar foliation should be re-evaluated after more appropriate analyses are performed.*

These methodological suggestions are very helpful. We agree that both the anterior commissure analysis and the assessment of cerebellar foliation should be re-evaluated to enable more anatomically and quantitatively appropriate comparisons across species.

Anterior commissure:

We agree that the current analysis, in which AC area was measured from the coronal section showing the largest cross-sectional profile and normalized to whole-brain area in the same section, may be influenced by differences in brain geometry and section orientation among species. In the revised manuscript, we will re-evaluate the method used to quantify AC size, including measurements from sagittal or midsagittal views where anatomically appropriate. We will also examine normalization against volumetric measures, such as total brain or telencephalic volume, rather than relying solely on a single-section whole-brain area. The corresponding results and interpretations will be revised accordingly.

Cerebellar foliation:

We also agree that our current branch-counting approach should be considered in relation to established quantitative measures of avian cerebellar foliation. In the revised manuscript, we will evaluate whether the cerebellar foliation index described by Iwaniuk et al. (2006), or a comparable standardized measure applicable to our midsagittal MRI datasets, can be used to re-analyze cerebellar foliation. This will also allow us to place our observations more directly

in the context of the larger comparative datasets reported previously, including that of Cunha et al. (2021).

Importantly, we recognize that cerebellar foliation is strongly influenced by allometric and phylogenetic factors. We will therefore re-evaluate the interpretation of interspecific differences in cerebellar foliation in light of brain/body size relationships and the existing comparative literature. In particular, we will revise the interpretation of the pronounced cerebellar foliation observed in penguins and other species and avoid attributing these differences directly to locomotor or sensorimotor specialization unless supported by the revised analyses.

https://doi.org/10.7554/eLife.112415.1.sa0